AN ABSTRACT OF THE THESIS OF

Robert F. Melendy for the degree of Master of Science in Mechanical Engineering presented on September 9, 1994. Title: Noncontact Measurement of Shaft Torsional Displacements by Optical Means

Abstract approved: Clarence A. Calder

Clarence A. Calder

An optical diagnostic system capable of measuring angular displacements in a torsionally loaded shaft through noncontact means has been developed. Conventional torsion diagnostic mechanisms must come in contact with the shaft to be analyzed. The signal-to-noise ratio response of conventional systems is compromised by dirt and wear. Another consequence of these devices is that the shaft being diagnosed must be cut in half to implement the mechanism.

In this work, the shaft angle of twist (ϕ) is measured utilizing precision optics and HeNe laser light. Accuracy in the placement and orientation of mirrors on the shaft surface is shown to be crucial, since precise bending of the laser light is required to effectively measure twisting distortions.

A CdS photoresistor was augmented with a high gain operational amplifier for light sensing. This system was then implemented as the receiving source of optically measured torsional displacements. Experimental results confirm that the voltage response of the amplifier varies linearly with ϕ. It is shown that the amplifier output voltage varies as a function of the amount of optical energy received from the shaft reflected laser light. The amount of optical energy transmitted to the circuit is dependent on the angle of twist in the shaft. The system performs these tasks without any physical contact between the laser source, shaft, or the photocircuitry.

Noncontact Measurement of Shaft Torsional Displacements by Optical Means

by

Robert F. Melendy

A THESIS

submitted to

Oregon State University

in partial fulfillment of
the requirements for the
degree of

Master of Science

Completed September 9, 1994
Commencement June 1995

TABLE OF CONTENTS

TABLE OF CONTENTS (Continued)

LIST OF FIGURES

LIST OF FIGURES (Continued)

LIST OF FIGURES (Continued)

LIST OF TABLES

Noncontact Measurement of Shaft Torsional Displacements by Optical Means

Chapter 1. Introduction

1.1. Background and Motivation

An important diagnostic technique for marine manufacturers and the electric power industry is the determination of torque in a rotating shaft. Currently, there exists a need for a more efficient and inexpensive method for measuring torsional displacements in the shaft used to transfer power from a steam turbine to an electric generator. When power is transmitted by the turbine, the linking shaft must undergo a torsional twisting through an angle which is proportional to the transmitted torque. Measuring the resultant angle of twist is a difficult diagnostic task because the changes in shaft shearing strains are very small and occur at rapid rates.

The measurement of strain and torque in such instances is certainly not a new development. One current practice of torsion diagnostic testing involves dividing a shaft and permanently installing a $6,000 in-line transducer to link the two parts. This necessitates turbine shut down and the disassembly of other machine parts so that the torsion diagnostic unit can be fitted over the shaft. This downtime accumulates due to periodic maintenance and the replacement of worn and dirty parts, which seems to conflict with the demand for increased productivity. Yet such labor tasks are unavoidable to help maintain an accurate operation of sensing and transmitting torque transduced signals (e.g., a good signal-to-noise ratio must be preserved). The expense and inefficiencies involved in employing current torque sensors has established the need for a system capable of providing a signal proportional to the torque carried by a shaft, while avoiding the problems associated with present in-line diagnostic methods.

1.2. Literature Review

The two principal functions of a noncontact torque sensor are (1) the detection of angular twisting distortions in a shaft subjected to a static or dynamic torsional load, and (2) conversion of the elastic response into electrical information that can be spatially transmitted to a remote receiver-demodulator unit (RD). The RD circuitry must be designed to respond to small changes of the transmitted signal which correspondingly change with shaft torsional displacements.

The fundamental idea is to avoid contact between the shaft and the torsion diagnostic unit unlike currently marketed torque sensors which come in direct contact with the shaft. Nevertheless, current devices effectively measure torsional displacements in stationary and nonstationary shafts. This section gives a detailed discussion of the operation of currently used devices.

Currently marketed torsion diagnostic mechanisms can be divided into two major categories: (I) In-line rotating shaft torque sensors and (II) windup torque sensors. The former is classified as a device which is placed directly *in series* with the shaft, whereas the latter may be viewed as a system *suspended* from the shaft. Those types which correspond to (I) are subclassified into four groups: (A) The classical slip-ring construction; (B) the rotary transformer type; (C) the Torsional Variable Differential Transformer™ (TVDT); and (D) the optical slip-ring type. The devices of category (II) are classified as phase shift torque measuring systems.

1.2.1. Type (I) Torsion Diagnostic Mechanisms (Series Configurations)

The first of the in-line rotating shaft torque sensors to be discussed is that manufactured by Lebow® products [1992] and is illustrated in Figure 1.2.1.1. This design is of the classical slip-ring construction and operates in the following manner.

A *strain gauge bridge* is composed of four gauges connected to four silver slip-rings mounted on a rotating shaft. Silver graphite brushes rub on these slip-rings and provide an electrical path for the incoming bridge excitation and the outgoing signal (either AC or DC voltages can be used to excite the strain gauge bridge). When rotating in a strong magnetic field, the slip-ring system will generate small extraneous voltages which are amplified by a readout circuit. Because of millivolt signal levels produced by the strain gauge bridge, the rings and brushes must be periodically cleaned to maintain a satisfactory signal-to-noise ratio of the bridge elastoelectric response signal.

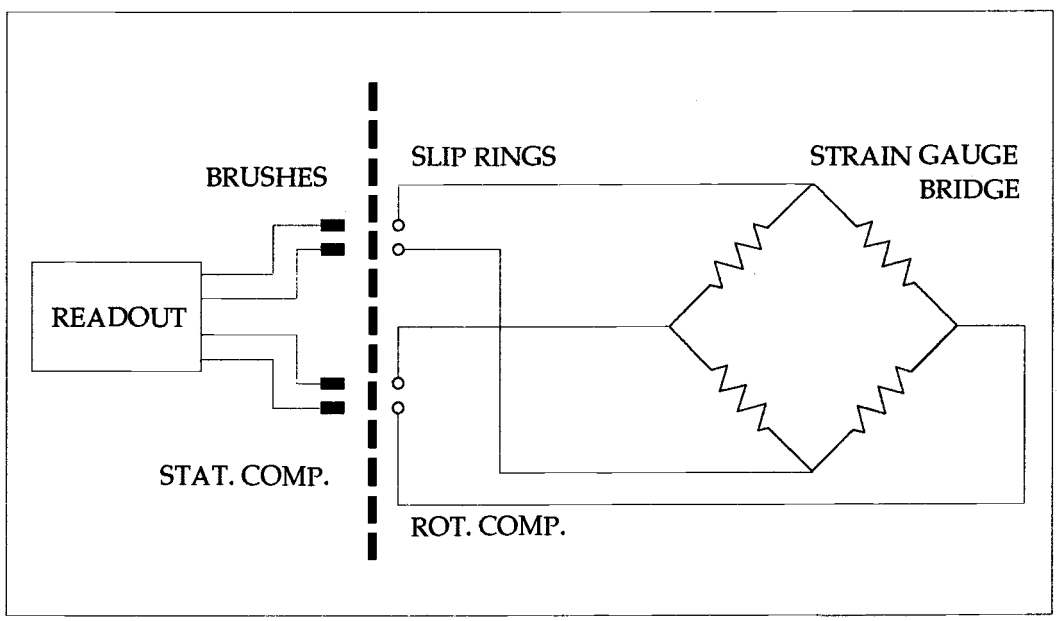

Figure 1.2.1.1. Slip-ring rotating shaft torque diagnostic system by Lebow®.

The second of the in-line rotating shaft torque sensors to be discussed is also manufactured by Lebow® [1992] and is illustrated in Figure 1.2.1.2. This design is configured as the rotary transformer type. In general, rotary transformers differ

from conventional transformers only in that either the primary or secondary winding is free to rotate. One transformer is used to transmit the AC excitation voltage to the strain gauge bridge and the second transformer transfers the output signal to the nonrotating part of the torque transducer. Thus, two transformers take the place of four slip-rings, and no direct contact is required between the rotating and stationary elements of the transducer.

Lebow® describes the transformers as a pair of concentrically wound coils with one coil rotating within or beside a stationary coil. Magnetic lines of flux are produced by applying a time varying voltage to one of these coils. A high-permeability core resides between the windings, thereupon concentrating magnetic flux and improving coupling between the coils. There is a gap in this core to allow the passage of a support member for the inner rotating coil; this particular geometry

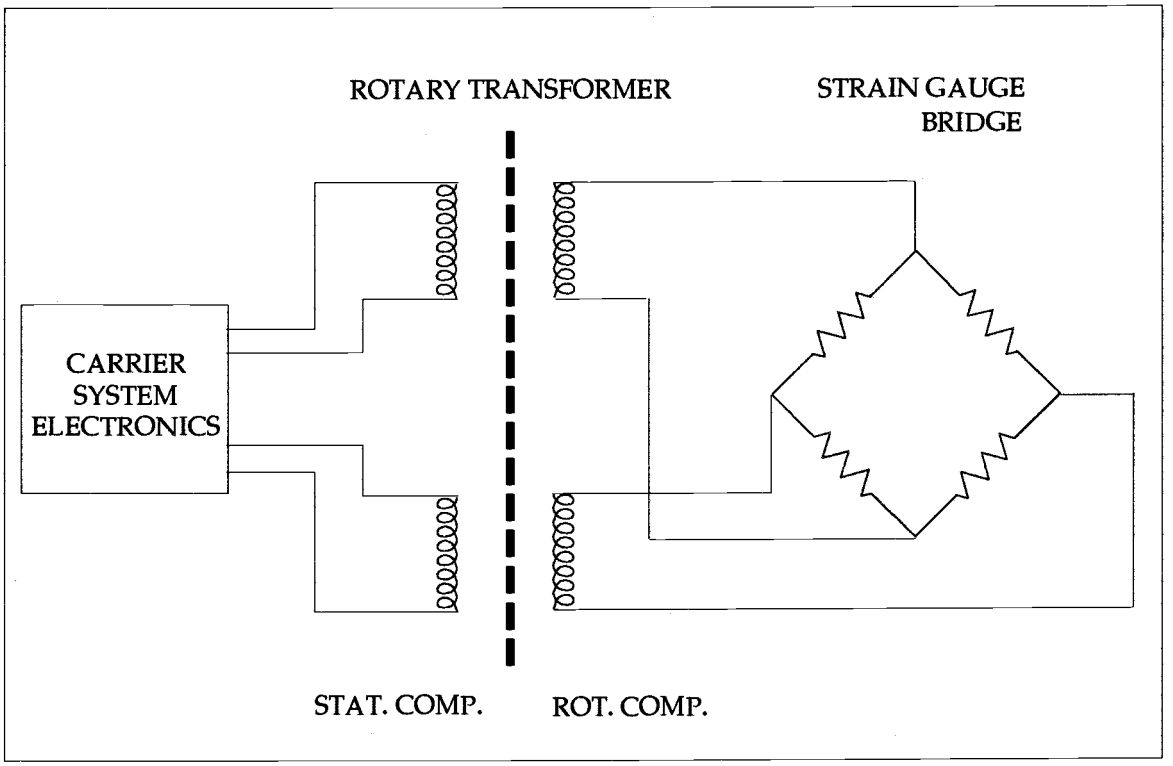

Figure 1.2.1.2. Lebow's® rotary transformer rotating shaft torque sensing system.

(Lebow® Pat. No. 3,611,230) enables the transformer to exhibit a high coefficient of coupling. Eaton Corporation [1992] suggests purchasing a suitable carrier instrument to be used with the rotary transformer torque sensor which provides AC excitations in the range of 3 kHz (e.g., Lebow® model 7540).

The third type of torque sensor investigated was the Torsional Variable Differential Transformer™ (TVDT). This design is illustrated in Figure 1.2.1.3 and is manufactured by Lebow® products. The TVDT™ design measures the angular deflection of a shaft under an applied torque by means of a magnetic field. A shaft made of nonmagnetic material has attached to it three tubular pieces of a magnetic material (A,B,C) with gaps at 45° to the shaft axis. A torque applied to the ends of the shaft will cause one of the gaps to close and the other to open; this action causes

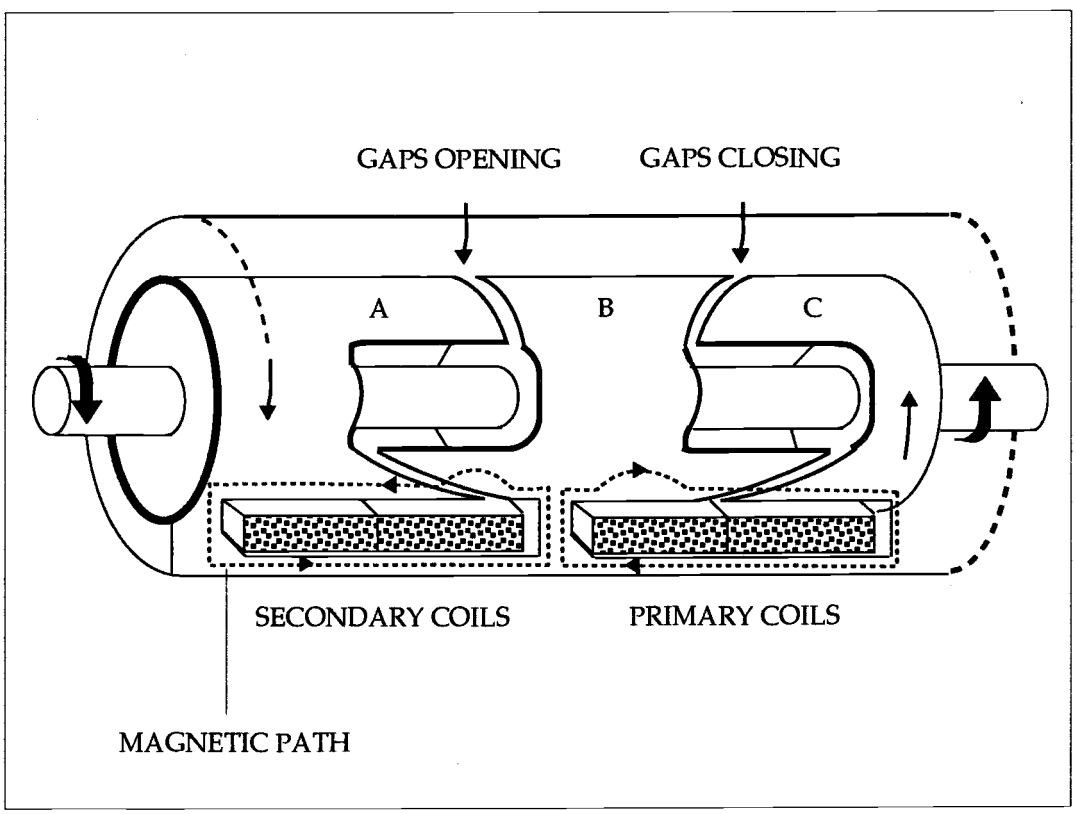

Figure 1.2.1.3. The Torsional Variable Differential Transformer™ by Lebow®.

the magnetic reluctance in each gap to correspondingly increase and decrease, respectively. Blitzer [1974] states that an AC voltage applied to a primary coil will necessarily induce a voltage in a secondary coil. Thus, as the shaft is twisted, one secondary coil will show a voltage increase and the other a proportionate decrease. These secondary voltages are transmitted to a circuit which adds the signals together to produce a signal with a polarity that indicates the direction of torque and with a magnitude that is proportional to the torque. Eaton Corporation [1992] claims that a specially designed carrier instrument is needed to supply the power and condition the signal in a system of this kind.

The fourth and last of the in-line rotating shaft torsion sensors is the optical slip-ring type. Such a device is manufactured by Litton® Fiber Optic Products [1994] and is illustrated in Figure 1.2.1.4. Litton's® fiber optic rotary joints are fiber optic slip-rings capable of transferring strain signal data between rotating and stationary components. Unlike conventional torque monitors, this type of device is a self-contained capsule which includes ball bearings and one meter of fiber optic cable on

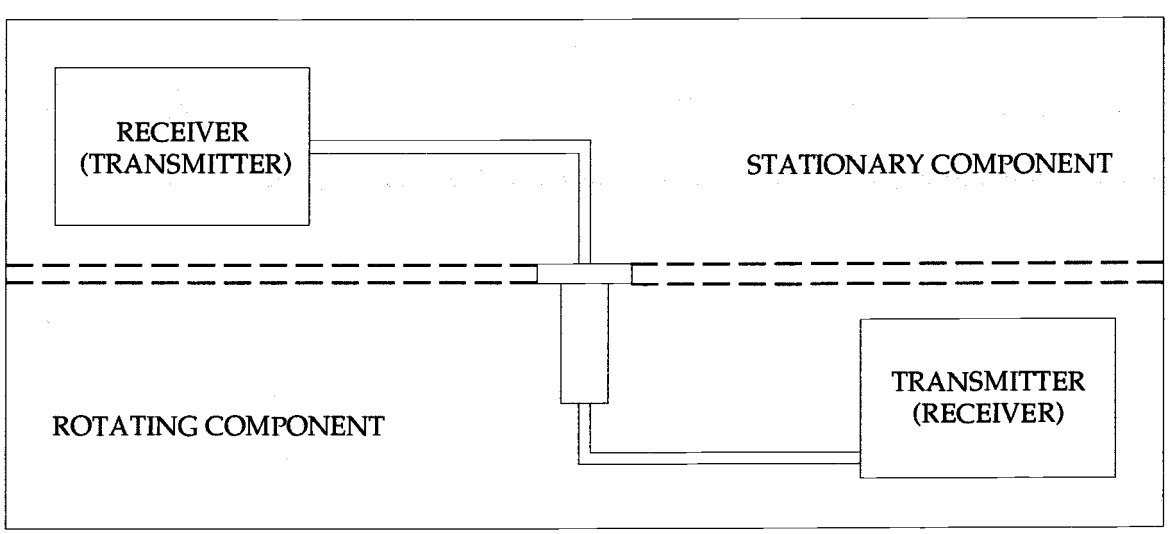

Figure 1.2.1.4. Litton's® fiber optic rotary joint (slip-ring) torsion diagnostic system.

each end of the capsule. Classical slip-ring circuits must be hybridized with the fiber optic rotary joint because electrical current is needed to power internal photoelectronic circuits. The operating wavelength (λ) of this device lies in the range of $0.83 \leq \lambda \leq 1.30$ microns.

1.2.2. Type (II) Torsion Diagnostic Mechanisms (Phase Shift Configuration)

The type (II) torsion diagnostic mechanism of interest is manufactured by Ono Sokki® Co., Ltd. [1994] and is called the Phase Difference Detection System™ (PDDS). The chief component used to describe the principle of operation of this system is called the torque transmission shaft and is illustrated in Figure 1.2.2.1.

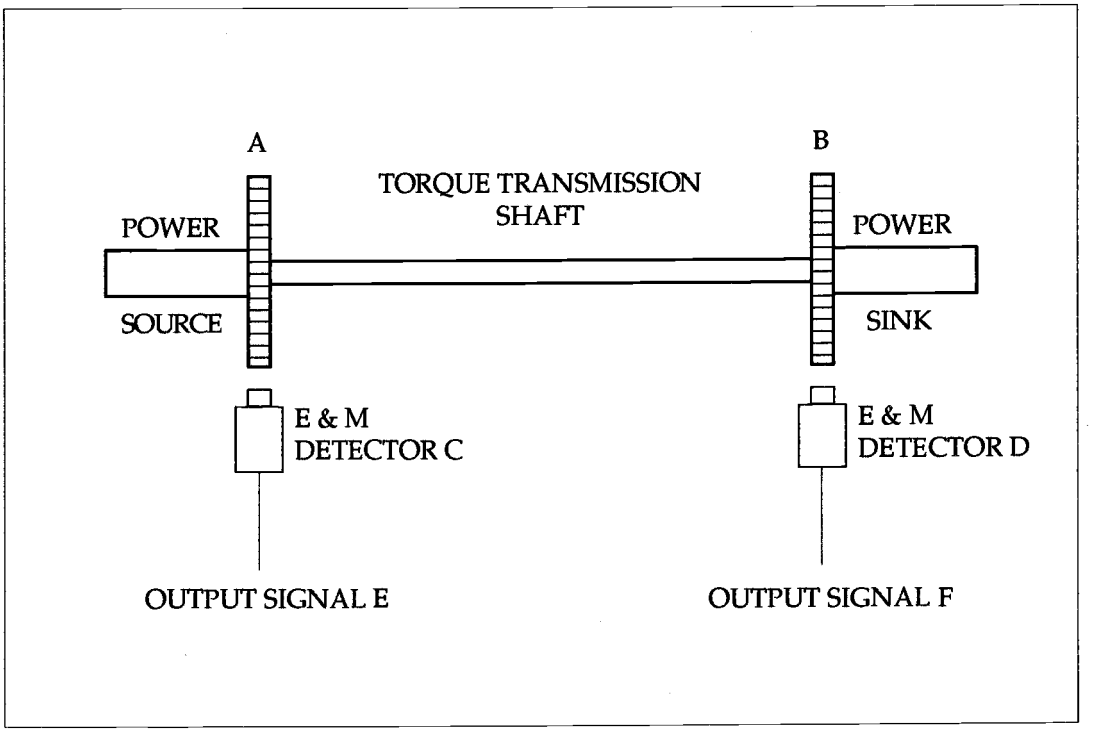

Figure 1.2.2.1. PDDS torque transmission shaft with electromagnetic sensors.

The PDDS mechanism operates in a manner similar to conventional strain gauge diagnostic units in that torsional displacement or *windup* is converted to a proportional electrical signal. Two pulse-type magnetic sensors are employed, one at either end of the torque transmission shaft. As shown in Figure 1.2.2.1, a series of evenly spaced discontinuities (similar to gear teeth) are located at either end of the shaft and are labeled gears A and B. Directly under these gears are a pair of electromagnetic detectors which are labeled C and D.

When the shaft of Figure 1.2.2.1 is subjected to a torsional load, it will twist through an angle proportional to the magnitude of the applied torque, so that the teeth of gears A and B will be displaced in relative position by an amount equal to the shaft angle of twist, ϕ. Since sensors C and D generate AC voltages with waveforms that track the rotation of gears A and B, the phase difference between the output signals will vary in proportion to ϕ. In other words, twisting of the shaft generates a phase shift between the sinusoidal outputs from each of the electromagnetic sensors. The applied shaft torque can therefore be determined by measuring the phase difference between the two AC response signals generated by sensors E and F.

1.3. Extended Literature Search: The F-2003 Single-Channel Telemetry System

The F-2003™ single-channel telemetry system developed by Binsfeld Engineering Inc. [1993] is designed to measure rotational torque in a spinning shaft while avoiding the problems associated with the traditional in-line diagnostic methods discussed in section 1.2. According to a description published by *Mechanical Engineering Magazine* (May 1993), the F-2003™ system operates in the following manner.

A torsion-sensitive strain gauge ($\mathcal{G}$) is bonded directly to a rotational shaft by a typical cyanoacrylate adhesive. Upon deformation, the elastoelectric response of the gauge is detected and processed by a battery-powered F-1001™ transmitter, $\mathcal{T}$. This transmitter is securely strapped to the shaft and is connected to the strain through a pair of short wires.

As the shaft experiences variations in torsional loads, the resistance of the strain gauge changes, thereupon generating a torsionally transduced voltage signal. This elastoelectric response is converted by the transmitter circuitry to radio frequencies in the 88-to-100 MHz band; this band of frequencies ($\mathcal{F}$) is then transmitted to a remote receiving antenna ($\mathcal{A}$) located at an isolated site. This antenna is connected by a coaxial cable to a Binsfeld F-2003™ Receiver Demodulator ($\mathcal{RD}$); the $\mathcal{RD}$ unit has a built-in FM receiver that converts the radio signal into an audio frequency response. An operator has the option of switching on a speaker so that an audio tune corresponding to changes in torque can be observed; increases in the speaker response reflect a positive torque and decreases in the tone correspond to a negative torque.

A demodulator circuit ($\mathcal{D}$) converts the audio signal into a DC voltage appropriate for output to a chart recorder, $\mathcal{CR}$. The resultant hard copy is a record of the real-time shaft torque measurement. Thus, the F-2003™ diagnostic system operates according to the principle of telemetry, and can be used on rotating shafts with diameters from 1 to 22 inches. Figure 1.3.1 is a schematic which summarizes the operating principle of this system.

1.4. Research Objectives

Most of the torsion diagnostic systems investigated require sophisticated measuring instruments in order to demodulate the information about the torque.

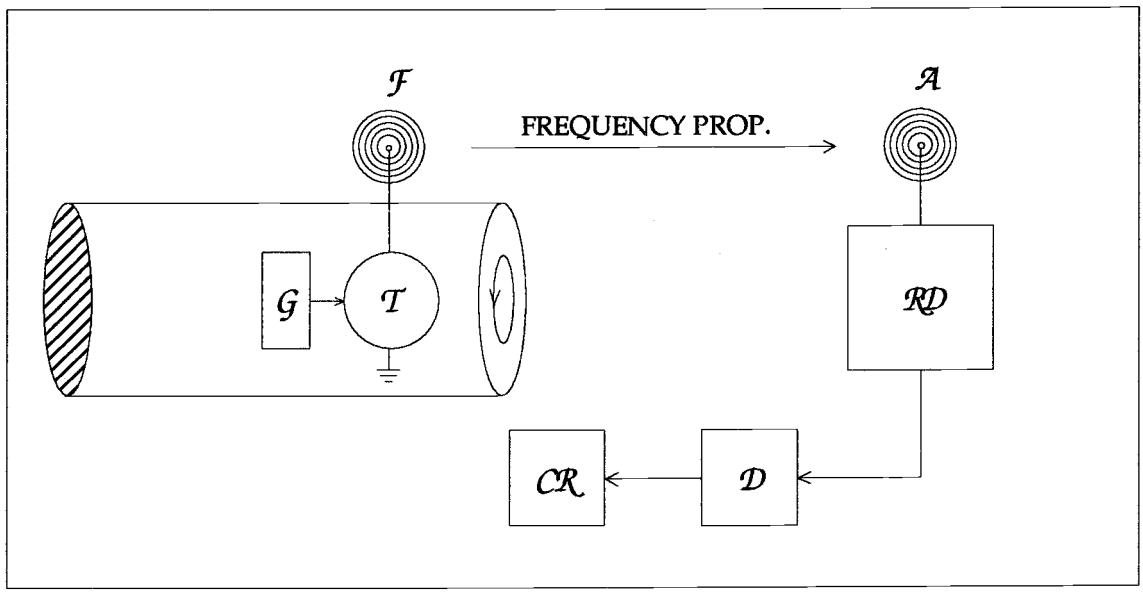

Figure 1.3.1. Basic operating principle of the F-2003™ torsion telemetry system.

The accuracy and precision of the torsionally transduced response signals generated by such devices decrease with time as moving parts accumulate dirt and wear out. Simple maintenance schedules for these systems necessarily create plant downtime since shaft disassembly is usually required.

The F-2003™ telemetry system removes the problem of sending gauge elastoelectric response signals across a mechanical interface, the accuracy of which is compromised by dirt and wear. But this system also requires special electronic instrumentation. In addition, attenuation phenomena via coaxial lines attenuate the elastoelectric response signals generated by the strain gauges.

Another possible approach is to optically measure and transmit information on torsional displacements. In this study, the focus is on the development and experimental observation of an optical system which can measure variations in the angle of twist (ϕ) in a torsionally loaded shaft through transmission to a photosensitive configured network. The objectives are: (1) To use a low power laser beam to continually and repeatedly track changes in the angle of twist in a shaft subjected to a static torque; (2) to transmit the laser light to an inexpensively designed electronic

circuit capable of responding to small changes in the amount of optical radiation energy $\mathcal{E}$ absorbed by a sensor, such that $\mathcal{E} = \mathcal{E}(\phi)$; and (3) to derive an empirical expression relating the shaft angle of twist as a function of the photosensitive circuit response, such that:

$$\phi = \phi(V_{Out}) \tag{1}$$

where ϕ is the angle of twist of a torsionally loaded shaft and V_{Out} is the corresponding output voltage of the circuit. In other words, the proposed circuit must be capable of an output response that varies in voltage depending on the amount of laser radiation absorbed by a photosensor in the network; in turn, the energy absorbed by the sensor will be dependent on ϕ (this will be thoroughly discussed in Chapter 3). Figure 1.4.1 illustrates the mechanical/optical/electronic conversion process of the proposed system.

The remaining chapters of this thesis are arranged as follows: Chapter 2 will discuss the process of interfacing laser light with twisting distortions in a solid circular shaft. Basic relationships from mechanics of materials will be employed and correlated with relations from physical optics. Chapter 3 will deal exclusively with the design of the optoelectronic network. Chapter 4 presents: (1) The experimental procedure for implementing the optical measuring system; (2) observation of the measured voltage response of a photosensitive configured amplifier to changes in shaft torsional displacements; and (3) discussion of experimental results. Conclusions and recommendations for future research are presented in Chapter 5.

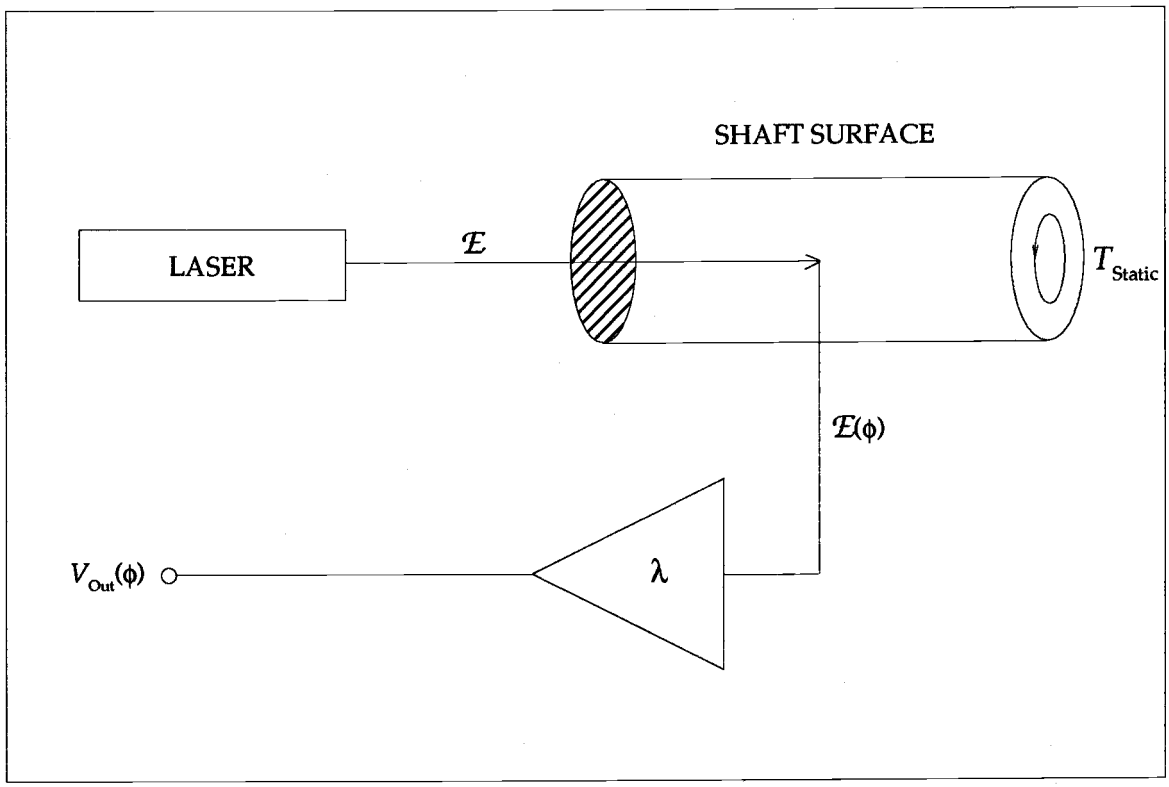

Figure 1.4.1. Proposed mechanical-to-optoelectronic conversion process.

Chapter 2. Linear Displacement of a Reflected Optical Beam as Related to Shaft Angle of Twist

2.1. Introduction

In order to describe how laser light can be made to measure the angle of twist in a torsionally loaded shaft, an understanding of how linear displacements of a reflected optical beam change in proportion to the shaft angle of twist is essential.

First, the mechanical response of a shaft to a torsional load must be elastic. Second, means must be obtained to force the laser light to track angular distortions caused by a state of pure shear. Achievement of this process will lead to the development of an empirical expression relating the angle of twist of a shaft to the displacement of the returning optical beam. It is assumed that displacements of the optical beam will be linear for small values of ϕ. This will be experimentally verified.

2.2. Torsional Loading of a Solid Circular Shaft

Throughout this paper, torsion relations as described by Gere and Timoshenko [1962] will be used as a theoretical basis. In the following analysis and all subsequent experimental work, it will be assumed that all shaft specimens will remain within the range of their elastic limits during and after the removal of torsional loads.

Consider the solid circular elastic shaft of Figure 2.2.1 which is used to transmit torque T from a steam turbine to an electric generator. Specifically, it is of interest to analyze the effects of the elastic twist caused by shearing stresses between test planes P_1 and P_2. Let the amount of shaft length between these two planes be set at $\Delta x = 3$ inches. This incremental segment was chosen since it is the actual exposed length observed in most turbine-generator systems (the torsion diagnostic mechan-

isms discussed in Chapter 1 occupy this length). In the development of the proposed optical system, twisting deformations in this region will be analyzed.

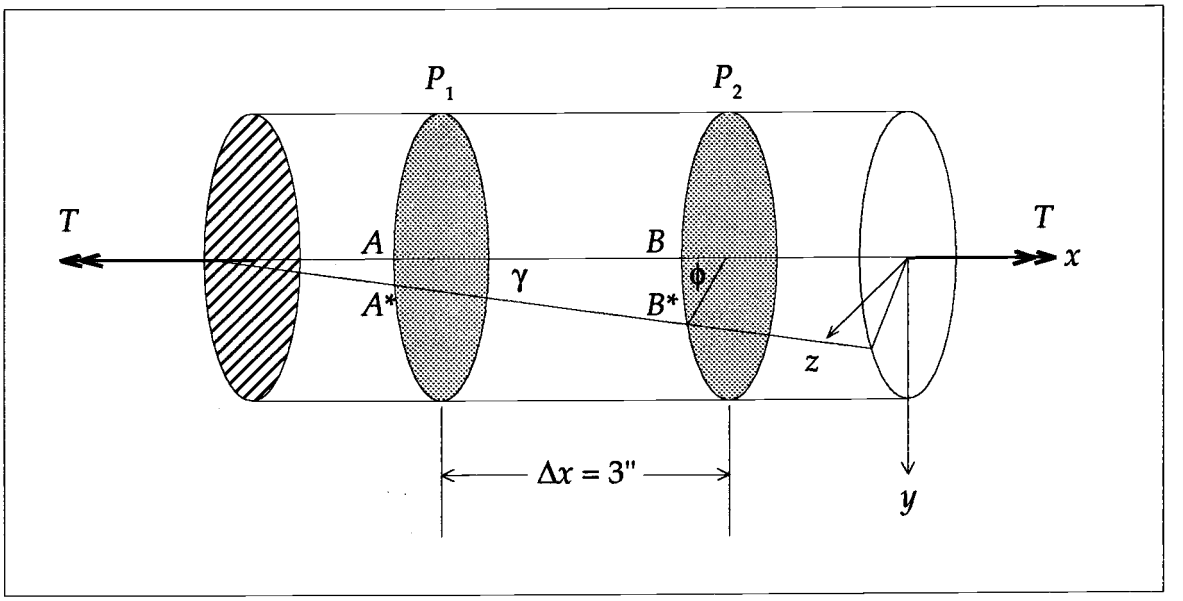

Figure 2.2.1. Torsional loading of a solid circular elastic shaft and elastic response.

Assuming that the shaft of Figure 2.2.1 is subjected to a pure shear and that the response of the material is consistent with Hooke's law, the shearing strain γ can be calculated by the analytical expression:

$$\gamma = \frac{Tr}{GJ} \tag{2}$$

where T is the applied torque which generates a state of pure shear, J is the polar moment of inertia, r is the shaft radius, and G is the shear modulus. Since Young's modulus E and Poisson's ratio ν are known, G can be calculated by the equation:

$$G = \frac{E}{2(1+\nu)} \tag{3}$$

The angle of twist in segment P_1P_2 is obtained as:

$$\phi = \frac{T\Delta x}{GJ} \tag{4}$$

where ϕ represents the angle of twist between planes P_1 and P_2.

2.3. Optical Measurement Approach

The fact that a laser generated beam must follow changes in the angle of twist of a torsionally loaded shaft has provided the incentive for allowing the source light to fall incident on plane P_1, and to somehow reflect this beam to plane P_2. This must be performed in a manner which will allow an *intermediate* reflected optical beam to follow the shearing angle of the segment Δx as distortion due to twisting occurs.

The end goal is to utilize a *final* reflected optical beam as the information carrier of the value of ϕ. In order to compel laser generated light to measure changes in the angle of twist between planes P_1 and P_2, means must first be obtained to direct the source light incident on plane P_1 to plane P_2 in a repeatable and predictable manner.

Consider a vector $\boldsymbol{k}_i$ which designates the direction of propagation of a laser generated beam. Allowing this vector to reside in the x-z plane of the shaft along the negative z-axis (see the defined coordinate system in Figure 2.2.1), one can write:

$$\boldsymbol{k}_i = k\mathbf{e}_z \cos \Psi \tag{5}$$

which is the equation for a wave propagation vector $\boldsymbol{k}_i$ residing in the x-z plane at an angle Ψ with the positive x-axis.

If the incident source beam is directed at a mirror at plane P_1, then $\boldsymbol{k}_i$ will reflect at an angle determined by the angular position of the mirror with respect to the projecting optical beam. Figure 2.3.1 illustrates the reflection of the incident source beam by a mirror $\mathcal{M}_1$ with a surface normal $\boldsymbol{n}$ oriented at $\Psi = 45°$ with respect to the x-axis of the shaft. Thus, the resultant reflected optical beam can be characterized by an intermediate wave vector $\boldsymbol{k}_r$ at an angle of 90° with $\boldsymbol{k}_i$.

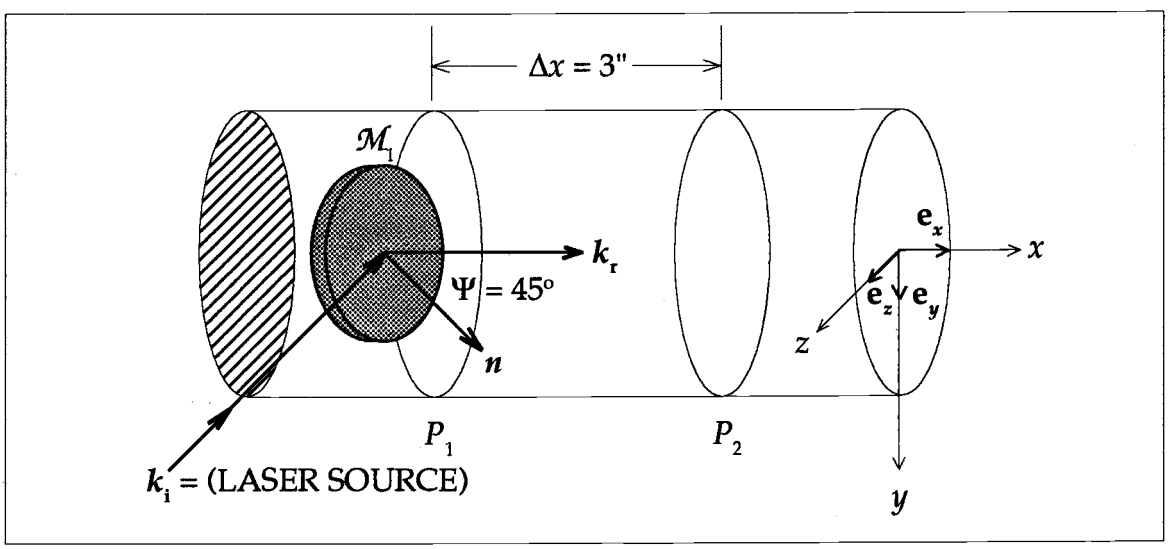

Figure 2.3.1. Creation of an intermediate reflected optical beam using a mirror $\mathcal{M}_1$.

The reflected optical beam vector $\boldsymbol{k}_r$ will reside in the x-z plane along the positive x-axis (towards plane P_2). Then:

$$\boldsymbol{k}_r = k\mathbf{e}_x \sin \Psi \tag{6}$$

Therefore, a second mirror $\mathcal{M}_2$ located at point B on the shaft surface (see Figure 2.2.1) could be used to reflect $\boldsymbol{k}_r$ at a 90° angle in the positive z-direction. The latter process will generate the final reflected optical beam, the magnitude and direction of which

is described by the vector $\boldsymbol{k}_f$. This effect is illustrated in Figure 2.3.2.

Upon the application of a torque, $\mathcal{M}_2$ will necessarily follow point B to B^* through an angle of ϕ (i.e., the angle of reflection of $\mathcal{M}_2$ will change in direct proportion to the angle of twist ϕ as "seen" by the vector $\boldsymbol{k}_r$). At point B^*, the vector $\boldsymbol{k}_f$ will have changed in direction but not in magnitude (i.e., $\mathcal{E}$ remains unchanged). This new vector representing a deformed state of the shaft will be symbolized by $\boldsymbol{k}^*_f$. Figure 2.3.2 shows that the angle between $\boldsymbol{k}_f$ and $\boldsymbol{k}^*_f$ is ϕ. Note from the illustration that the mirror at point A has not displaced. In reality, this is not the case; only the deformation at point B was exaggerated to illustrate that changes in the laser light will reflect at an angle of ϕ.

The irradiance of reflection of the final reflected optical beam can be expressed as:

$$I_{\text{Reflect}} = I^* \cos^2 (\Psi + \Delta\phi) \tag{7}$$

where I^* is the maximum irradiance reflected when $\Psi = 90°$ (i.e., the vector normal $\boldsymbol{n}$ is colinear to $\boldsymbol{k}_i$). Throughout this work, Ψ will always be equal to 45° with respect to any beam so as to produce the effect illustrated in Figure 2.3.2. The variable $\Delta\phi$ is the radial arc swept out by ϕ from point B to B^*; the length of this arc will be constrained by the photosensor dimensions (see Chapter 4). For all practical purposes, it will be assumed that this arc length is small enough to be approximated by a linear displacement, Δs. The exact value of Δs can be calculated by:

$$\Delta s = \int [1 + \phi'(x)]^{1/2}\, dx \tag{8}$$

The integral in (8) can be used to calculate the arc length of the path traced out by the angle of twist as reflected by the final optical beam, where $\phi'(x)$ represents the first

derivative of $\phi(x)$. Hence, the energy of optical radiation absorbed by the sensor will change according to $\mathcal{E} = \mathcal{E}(\Delta s)$.

The integral in (8) will not be solved analytically. Instead, Δs will be equated to an empirical function which relates the linear displacement of the final reflected optical beam as a function of the shaft angle of twist. This numerical approximation will be derived from experimental data (see Chapter 4).

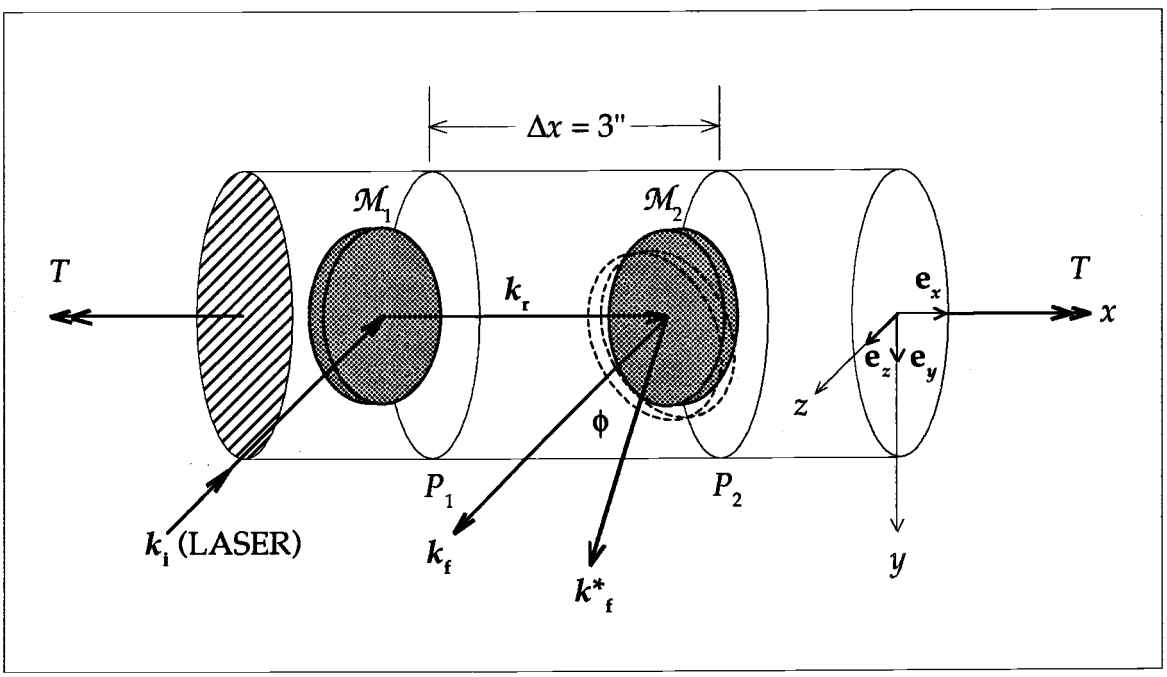

Figure 2.3.2. Illustration of the final reflected optical beam displacing linearly by Δs.

2.4. Closure

The problem of creating and effectively transmitting a reflected optical beam detectable by a photoconductor has been solved. A final task remains: Synthesizing a circuit capable of an output response that varies in voltage as a function of the incidence of optical radiation received, such that $V_{Out} = V_{Out}(\mathcal{E})$. Given that $\mathcal{E} = \mathcal{E}(\Delta s)$,

it is immediately evident that the voltage response of the circuit will change as a function of the beam displacement Δs. The subject of the next chapter is a circuit with this capability.

Chapter 3. Configuring an Operational Amplifier to Respond to Linearly Changing Optical Energy

3.1. Purpose

The basic requirement of the proposed photodetection circuitry is that it must be capable of an output response that varies in voltage as a function of the incidence of laser radiation received. Specifically, the laser radiation of interest is that contained in the final reflected optical beam k^*_f of Figure 2.3.2. As the angular displacement of the optical lever arm changes due to shaft torsional loads, then the intensity of the reflected laser light at any given instant in time can be expressed as the illumination surface density of energy absorbed by the photoconductive cell. Since variations in resistance of a photoconductive device are based on the amount of optical radiation impinged on the cell, then this type of element will be incorporated in the design of the proposed circuitry.

With respect to the relationship between the resistance R_λ for an intrinsic semiconductor device (i.e., a CdS photoresistor) and the energy of optical radiation $\mathcal{E}$ impinged on its active surface, a linearized model yields:

$$R_\lambda = R_0 \mathcal{E}^N \tag{9}$$

where R_0 is the resistance of a photoconductive cell when $\mathcal{E}$ is equal to 1 W-s. The superscript N is a dimensionless number that represents the slope of a straight line on a log-log resistance versus flux density graph; the numerical value of N can be calculated using the equation:

$$N = \frac{\ln(R_1/R_2)}{\ln(\mathcal{E}_1/\mathcal{E}_2)} \tag{10}$$

where R_1 and R_2 are the resistance values of a photoconductor resulting from incident radiation energies $\mathcal{E}_1$ and $\mathcal{E}_2$, respectively. In this work, a beam impinged on the active surface of a photoconductor at a position s_1 will mean that the cell is absorbing a radiation energy of $\mathcal{E}_1$. When this beam is deflected to position s_2 on the active surface, the energy will be $\mathcal{E}_2$, where $\mathcal{E}_2 < \mathcal{E}_1$. None of the variables expressed in equations (9) or (10) will actually be calculated; but knowing how to apply equation (9) in the design of a circuit that can convert a change in resistance to a change in current is essential. Realizing the extreme sensitivity of a CdS photoconductor to HeNe laser wavelengths (i.e., $\lambda_{HeNe} = 632.8$ nm), a CdS device will be used with of the photodetection-amplifying circuitry.

3.2. The Differential Amplifier Configuration

If the photoresistive response of a CdS device is to be augmented by a voltage generating circuit, then the output voltage of the candidate configuration must effectively respond to changes in the amount of optical radiation received by the CdS cell. Further, output sensitivity and magnitude of the voltage response are crucial considerations. Realizing that the operational amplifier can provide enormous voltage gains with the proper choice of input resistive loops, this device appears to be a good candidate in the interest of this work.

Consider the 741 op amp differential amplifier illustrated in Figure 3.2.1; this particular configuration contains a CdS cell as a feedback resistor in the noninverting circuit. This op amp will generate an output voltage that is proportional to the input current differential (Δi) to yield an output voltage that is related to illumination. Depending on the amount of laser light that falls incident on the CdS cell, a large mismatch between gains can result; because slight changes in the incidence of optical radiation can cause large changes in resistive values of the CdS cell, this gain

gain mismatch effect will be greatly amplified. For the inverting input (-), the gain magnitude is R_2/R_1, while the noninverting input (+) gain yields $1 + (R_\lambda/R_3)$. In either case, R_2 and R_λ are feedback resistors.

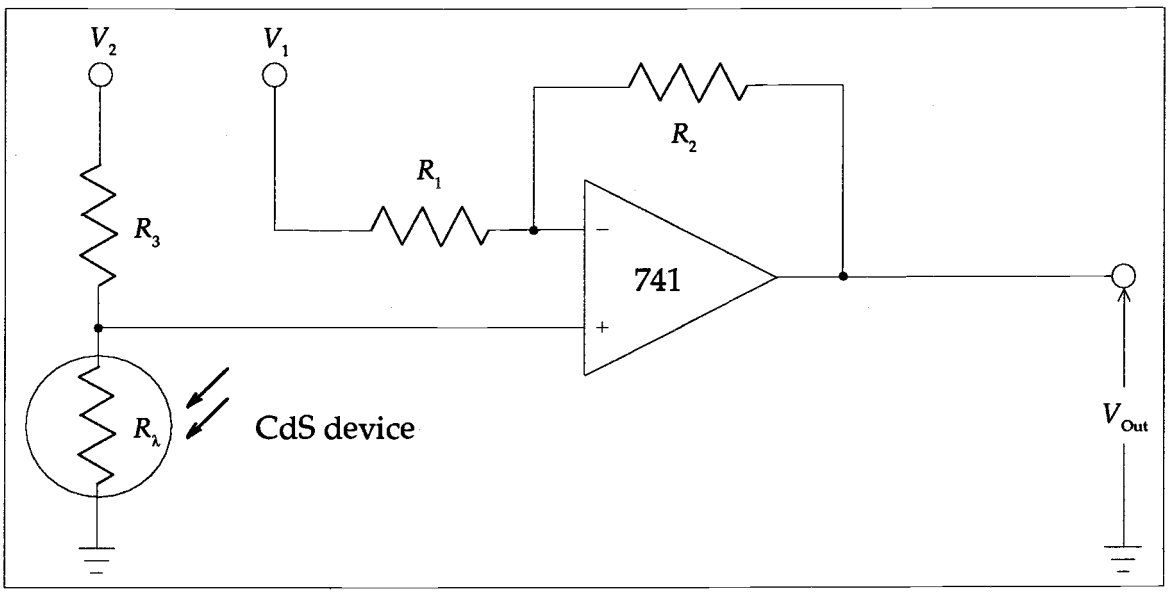

Figure 3.2.1. A differential amplifier with a CdS cell as a positive feedback resistor.

The output voltage of the op amp circuit illustrated in Figure 3.2.1 is expressed by the equation:

$$V_{Out} = -\frac{R_2}{R_1}V_1 + \left(1 + \frac{R_2}{R_1}\right)\frac{R_\lambda}{R_3 + R_\lambda}V_2 \qquad (11)$$

where V_1 and V_2 represent the bias voltages to the inverting and noninverting resistor loops, respectively. Substituting equation (9) into (11) yields:

$$V_{Out} = -\frac{R_2}{R_1}V_1 + \left(1 + \frac{R_2}{R_1}\right)\frac{R_0\mathcal{E}^N}{R_3 + R_0\mathcal{E}^N}V_2 \qquad (12)$$

Equation (12) can be used to draw the following conclusions: (1) The voltage at the

amplifier output will *increase* as the input illumination *decreases*. (2) The sensitivity of the output response can be adjusted by varying the value of R_2 (i.e., the gain will be affected). (3) The output voltage sensitivity to changes in input current through the noninverting terminal is very high; this implies that small variations in R_λ will greatly affect the magnitude of V_{Out}.

3.3. Integrating the Reflected Beam with the CdS Dependent Op Amp

With respect to Figures 2.3.2 and 3.2.1, a state of zero input torque to the shaft will mean that the final optical beam as reflected by $\mathcal{M}_2$ will contain the maximum amount of laser radiation energy as detected by the CdS device. In this instance, the energy absorbed by the detector will be represented by $\mathcal{E}_1$, and the circuit of Figure 3.2.1 will be calibrated such that $V_{Out} = 0$ volts. As the shaft undergoes torsional loading, changes in the angle of twist will displace the vector $\boldsymbol{k}_f$ until the last increment of light leaves the photoconducting surface of R_λ. At this point, the amount of laser radiation energy absorbed by the CdS device will be a minimum, and is represented here as $\mathcal{E}_2 = 0$ W-s. From equation (12), a state of $\mathcal{E} = 0$ W-s means that $V_{Out} = -(R_2/R_1)V_1$ or V_{Max}. Figure 3.3.1 illustrates how changes in the shaft angle of twist will induce this response in the CdS/amplifier scheme. It is relevant to note that the beam energy $\mathcal{E}$ does not change as the shaft is twisted; the symbols $\mathcal{E}_1$ and $\mathcal{E}_2$ represent two states of the energy absorbed by the CdS cell.

At this point, the only task remaining is the laboratory implementation of the combined systems illustrated in Figure 3.3.1. Specifics pertaining to the choice of optics, electronics, instrumentation, and shaft material and size are the subject of Chapter 4. Experimental results will also be presented here, followed by a discussion of the results.

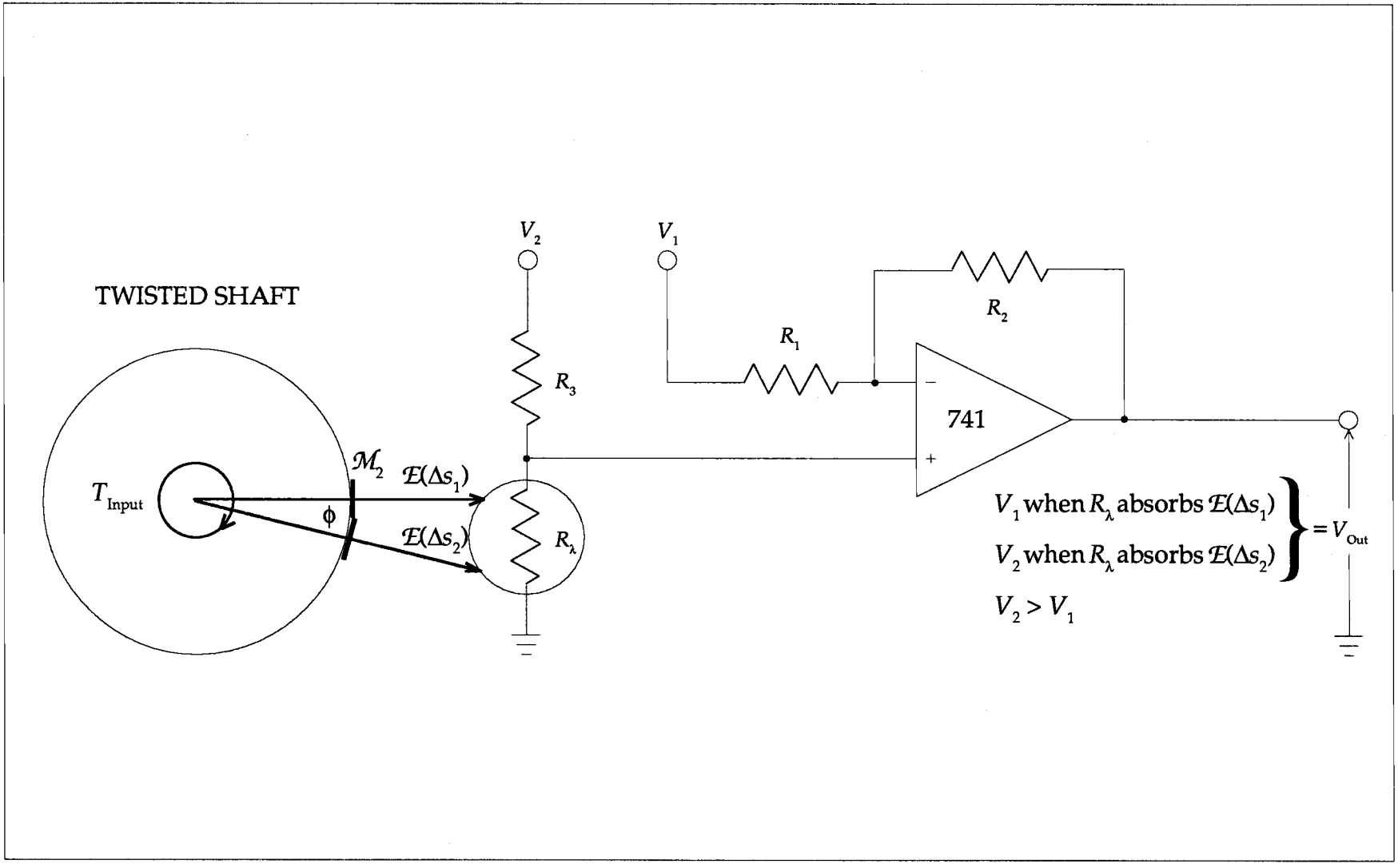

Figure 3.3.1. Amplifier voltage response as a function of optical energy absorbed by the CdS cell.

Chapter 4. Laboratory Implementation: Application, Results, and Discussions

4.1. Objectives and Strategies

The intent of this study has been to combine the mechanical, optical, and electronic components of Chapters 2 and 3 to form an operational system suitable for experimental observation. The system defined by Figure 3.3.1 was used to measure the angle of twist in one and two inch 1045 solid circular steel shafts, and a three inch 4140 solid circular steel shaft. Shear strain, amplifier output voltage, and optical beam displacement measurements were correlated with ϕ.

To effectively implement the system of Figure 3.3.1 and insure the reproducibility of experimental results, the following strategies were applied:

(1) Twisting deformations of each specimen were limited to the linear elastic region of the material.

(2) A system of lenses were used to render irregularities in the final reflected optical beam into a one dimensional line image.

(3) The exposed active surface of the CdS sensor was configured into an equilateral triangle; the beam width of the impinging line image was magnified to a width of at least 1.5 times that of the triangular base.

By enforcing items (1) through (3), a linear response of the amplifier to the shaft twisting angle was realized. These results were supported by iterative experimentation. It was verified that as R_λ continuously absorbed fewer amounts of laser radiation energy contained in a line image, a linear trend in the voltage response of the amplifier circuitry was produced. The CdS device implemented as R_λ is illustrated in Figure 4.1.1. The resistance range of this device is characterized by $250\,\Omega \le R_\lambda \le 12\,\text{k}\Omega$ constrained by $100 \le I \le 0.1$ footcandles, where I is illumination.

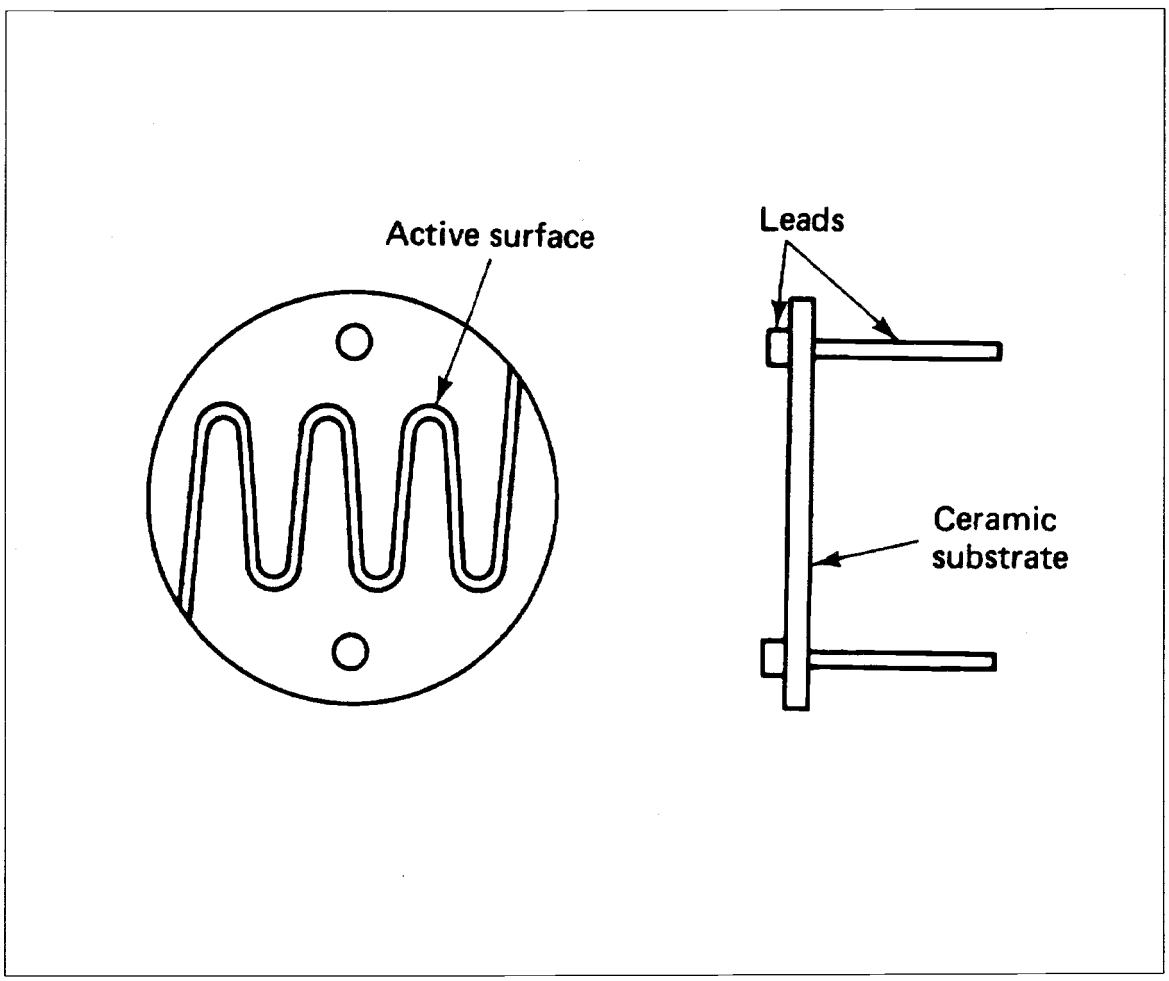

Figure 4.1.1. Two terminal CdS device implemented as R_λ.

4.2. Experimental Procedure

Figure 4.2.1 is an illustration of the complete experimental apparatus that was tested in the laboratory. Each shaft specimen was augmented with two Edmund Scientific 6.5 mm (≈ 1/4 inch) diameter first surface mirrors (i.e., $\mathcal{M}_1$ and $\mathcal{M}_2$). Using a typical cyanoacrylate adhesive, each mirror was affixed to the tip of a 45° bracket; in turn, the bracket was fastened to each shaft specimen yielding a mirror orientation of $\Psi = 45°$ to the shaft surface. The distance between the centers of the reflective and receiving surface of each mirror was $\Delta x = 3$ inches.

A MA-06-250TK-350Ω torsion sensitive strain gauge was bonded to the surface of each shaft specimen at midpoint. This was done so that: (1) Shear strain measurements could be recorded and correlated with the output voltage response of the amplifier circuitry; and (2) input torque could be calculated. Strain measurements were made using two Micromeasurements® P3500 strain indicators.

4.2.1. Shaft Mounting and Laser Alignment

Each shaft was mounted separately in a 60,000 in-lb_f Tinius Olsen™ torsion machine located in Graff Hall. The shaft mounting procedure was aided using a Melles Griot 1mW helium-neon (He-Ne) laser. The intent of the laser alignment procedure was to accurately produce the effect illustrated in Figure 2.3.2; that is to say, it was imperative that the optical beam returned by mirror $\mathcal{M}_2$ was reflected parallel to the laser source. The distance between the parallel beams was $\Delta x = 3$ inches (i.e., the distance between test planes P_1 and P_2). This effect was induced to insure that the final reflected optical beam followed the shaft angle of twist in a proportional manner. Regardless of the shaft diameter, the distance from the laser aperture to $\mathcal{M}_1$ was consistently held at 432 mm (≈ 17 inches).

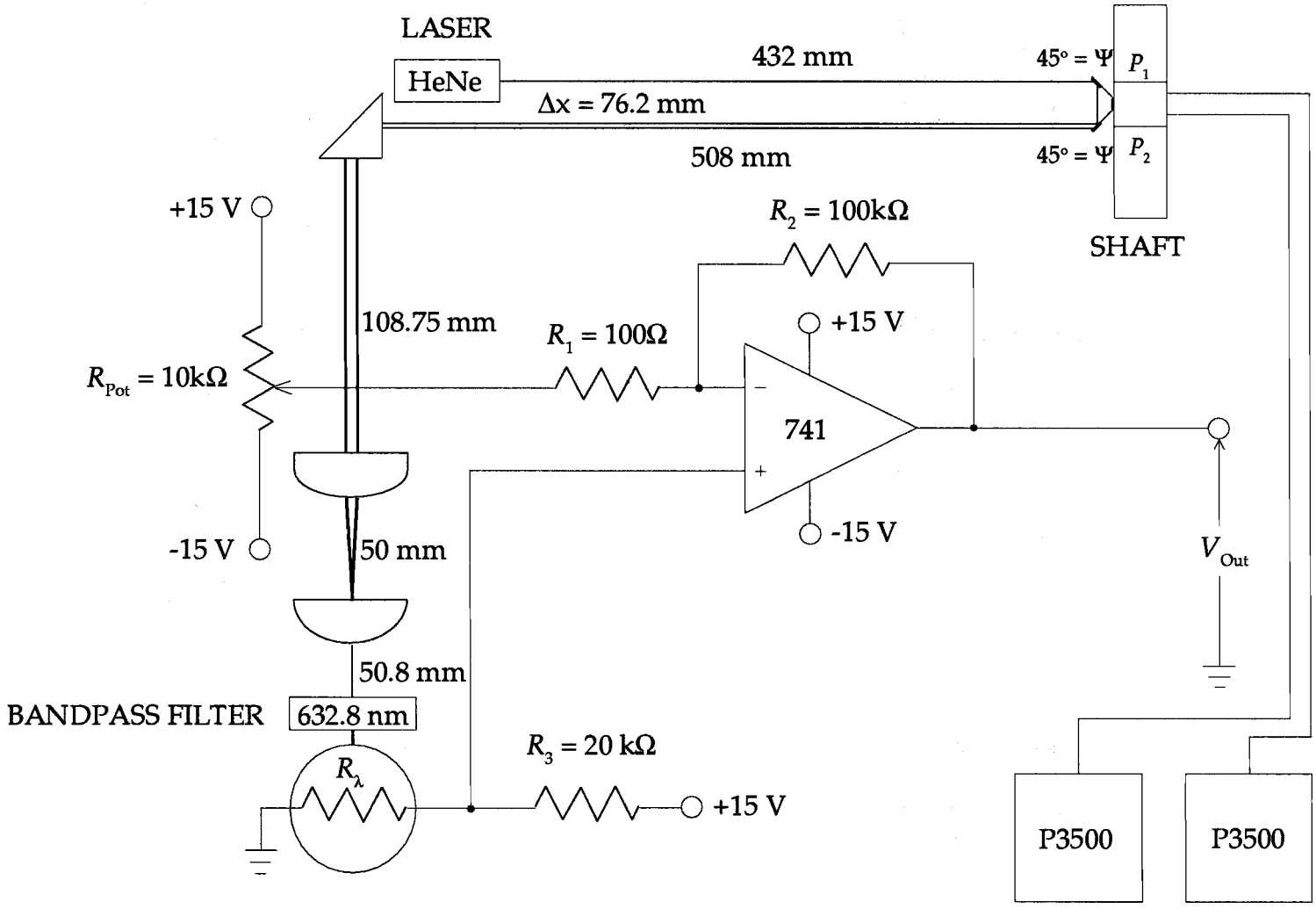

Figure 4.2.1. Schematic of test arrangement showing laser, lens assortment, CdS cell, and 741 amplifier.

4.2.2. Optical Beam Conditioning

An Edmund Scientific 312.5 mm^2 ($\approx$ 0.484 $inch^2$) right-angle prism was used to reflect the optical beam at a 90° angle downward (e.g., so as to impinge the laser light onto an easily accessible horizontal surface). The distance from $\mathcal{M}_2$ to the right-angle prism was consistently maintained at 508 mm (20 inches) to compensate for the different radii of each shaft. The height from the bottom of the prism to the horizontal surface was consistently held at 210 mm ($\approx$ 8.250 inches).

In all cases, the optical beam as reflected by $\mathcal{M}_2$ was not perfectly symmetric in shape and did not have a uniform intensity distribution. These irregularities were minimized by using the lens arrangement illustrated in Figure 4.2.1. A 25 mm diameter, 50 mm focal length PCX lens was used to condense the irregular beam shape. A 50 mm focal length cylinder lens transformed the condensed beam into a nearly uniform and intense elliptical-line. In all three cases, the elongated major axis of the elliptical-line image was consistently maintained at 16.7 mm ($\approx$ 0.656 inches).

4.2.3. Amplifier Circuit

A 741 op amp was powered by a Tektronix CPS250 triple output power supply. The CdS photoresistor of Figure 4.1.1 was used as R_λ. The diameter of this package is 11.11 mm (7/16 inches). A portion of the active surface was masked off with black electrical tape, leaving an exposed equilateral triangular surface area of 0.393 cm^2 ($\approx$ 0.061 $inch^2$). This procedure was performed to achieve maximum linearity between the displacement of the conditioned optical beam and the amplifier response. As a final precaution, an Edmund Scientific 632.8 nm laser bandpass filter was placed over the remaining exposed surface of the CdS cell. This filter blocked out all unwanted peripheral radiation except for that of the He-Ne light.

4.2.4. Calibration and Observation

After the reflected optical beam was aligned with the conditioning optics and the CdS cell, the 10 kΩ potentiometer was adjusted until the voltage at the amplifier output was $V_{Out} = 0$. At this point, an input torque was applied to the shaft until each strain indicator registered an output of 1 με and -1 με (i.e., a net result of $\gamma = 2$ με). Amplifier voltage response and strain measurements were simultaneously recorded and documented for each additional 1 με until the beam left the surface of the CdS device. These steps were repeated for each shaft.

4.3. Results

On the basis of consistently repeated strain measurements, voltage observations were averaged over a set of eight experiments to provide reasonable assurance of obtaining reproducible findings. Statistical analysis performed on raw voltage data confirmed repeatability through measures of central tendency and dispersion. A brief discussion concerning these results are presented in section 4.5.2.

With respect to a voltage arithmetic mean, linear regression analysis was used to develop a set of empirical equations relating ϕ and γ as a function of V_{Out}. Equations relating Δs as a function of ϕ were also generated. These equations form to standardize input torque calculations to a 1045 or 4140 steel shaft using the optoelectronic techniques of this study (i.e., without the use of the strain gauges).

Each relation was used to generate the curves of Figures 4.3.1 through 4.3.3. These plots illustrate the linearity of the optical beam displacement (Δs) as a function of shaft angle of twist (ϕ), and the linearity of the amplifier voltage response (V_{Out}) as a function of ϕ and γ. The symbols plotted on each curve are purely for visual identification; plots of raw data fitted with these same curves are in Appendix A.

$$\Delta s_1(\phi_1) := 5.212 \cdot 10^3 \cdot \phi_1 + 1.429 \cdot 10^{-4} \qquad \text{(1" diameter shaft)}$$

$$\Delta s_2(\phi_2) := 5.214 \cdot 10^3 \cdot \phi_2 + 1.364 \cdot 10^{-4} \qquad \text{(2" diameter shaft)}$$

$$\Delta s_3(\phi_3) := 5.211 \cdot 10^3 \cdot \phi_3 + 4.552 \cdot 10^{-5} \qquad \text{(3" diameter shaft)}$$

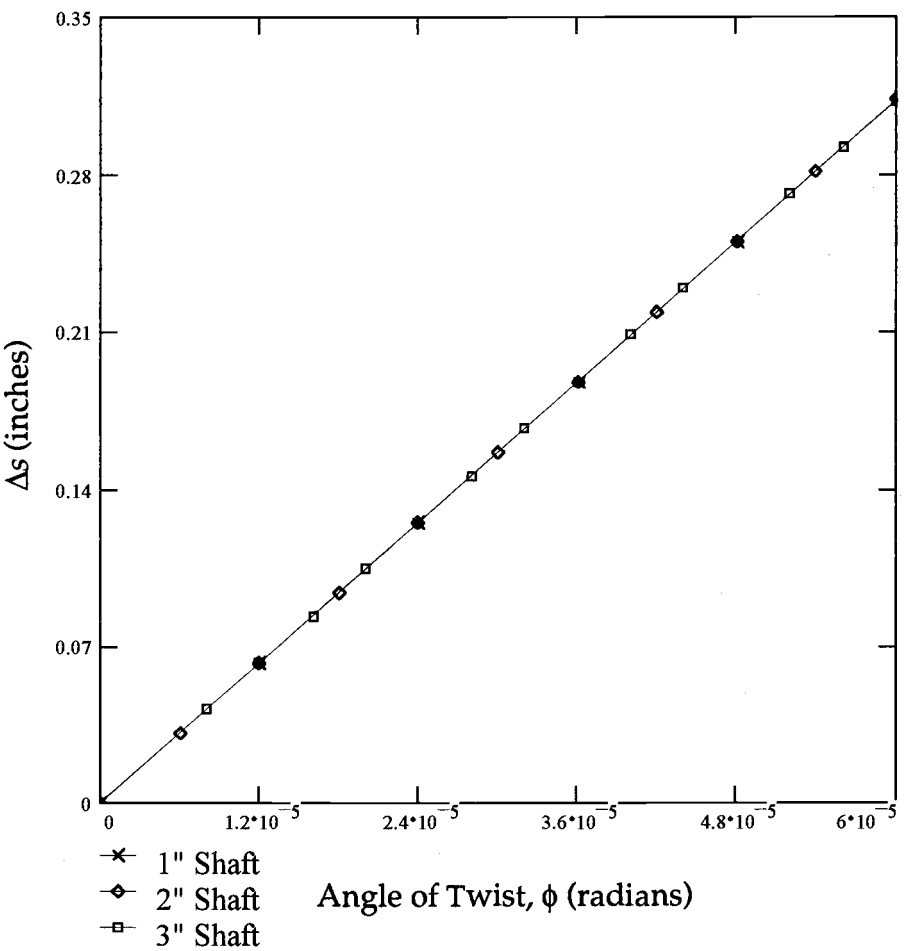

Figure 4.3.1. Linearized optical beam displacements (Δs) as a Function of ϕ.

$V_1(\phi_1) := 1.879 \cdot 10^5 \cdot \phi_1 - 0.274$ (1" diameter shaft)

$V_2(\phi_2) := 1.912 \cdot 10^5 \cdot \phi_2 - 0.374$ (2" diameter shaft)

$V_3(\phi_3) := 1.9 \cdot 10^5 \cdot \phi_3 - 0.24$ (3" diameter shaft)

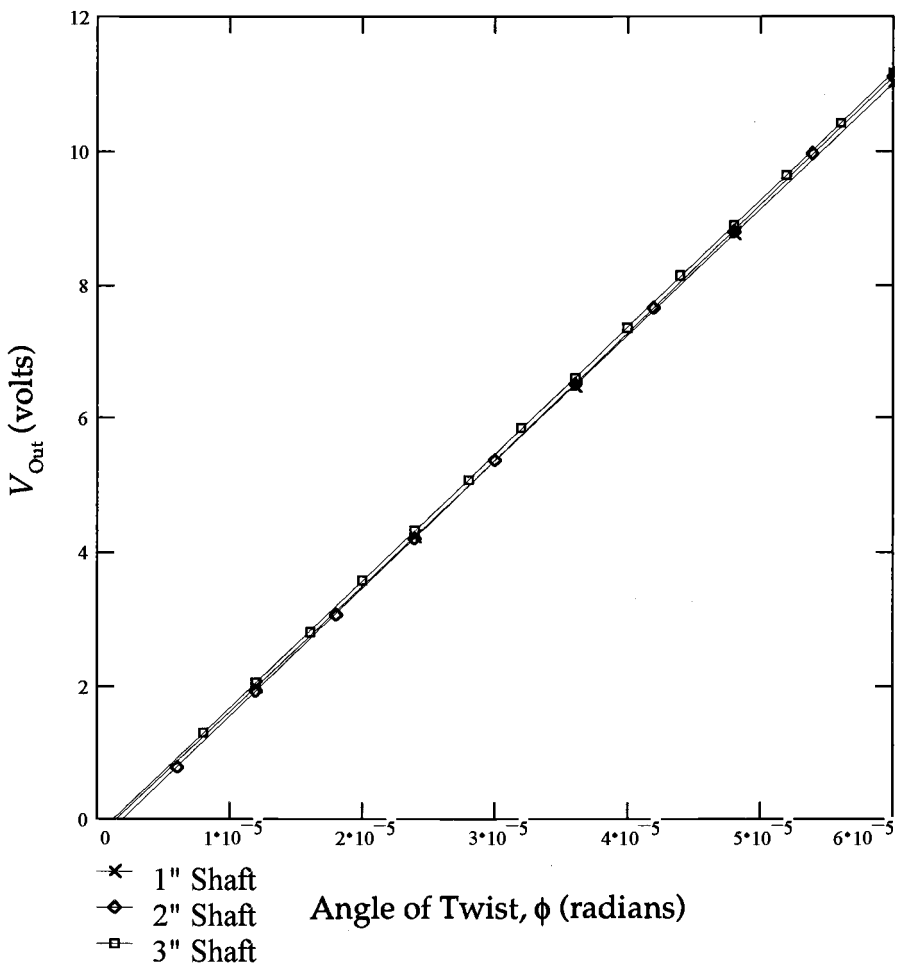

Figure 4.3.2. Linearized amplifier response (V_{Out}) as a Function of ϕ.

$V_1(\gamma_1) := 1.127 \cdot 10^6 \cdot \gamma_1 - 0.274$ (1" diameter shaft)

$V_2(\gamma_2) := 5.737 \cdot 10^5 \cdot \gamma_2 - 0.374$ (2" diameter shaft)

$V_3(\gamma_3) := 3.799 \cdot 10^5 \cdot \gamma_3 - 0.24$ (3" diameter shaft)

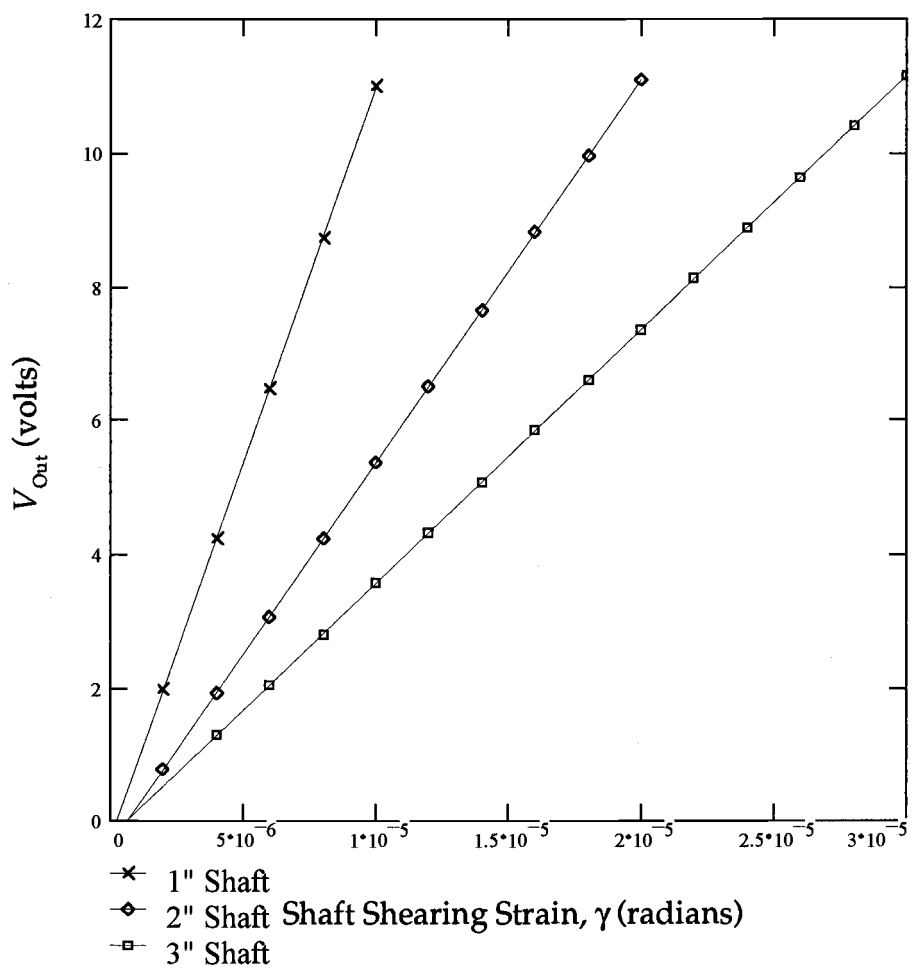

Figure 4.3.3. Linearized amplifier response (V_{Out}) as a Function of γ.

4.4. Discussion of Results

4.4.1. Linear Optical Beam Displacement Results

In performing optical beam displacement measurements, it was found that for each value of $\phi = 6.0(10^{-6})$ radians, a beam displacement of approximately 0.032 inches resulted. This was more or less a consistent finding for all shafts tested. The precision of these measurements were limited by visual observation; that is to say, the inability for one to discern displacements smaller than 0.032 inches. Hence, the curves of Figure 4.3.1 illustrate an acceptable idealization of these findings. The main purpose of this test was to build confidence that the linearity of $\Delta s(\phi)$ would induce a linear response in the amplifier.

The constraint of $0 \leq \phi \leq 6.0(10^{-5})$ radians resulted in a linear set of displacements constrained by $0 \leq \Delta s \leq 0.313$ inches; the limits of the latter inequality were pre-experimentally determined since 0.313 inches was the maximum limit that the beam could displace before leaving the sensor surface. In all three cases, the linearity of $\Delta s(\phi)$ serves to confirm the observed linear voltage response of the amplifier to displacements in the reflected optical beam (as seen in Figures 4.3.2 and 4.3.3).

Finally, the function $\Delta s(\phi)$ was applied as a numerical solution to the integral of equation (9). For the one, two, and three inch diameter steel shafts, the resulting numerical approximations yield, respectively:

$$\Delta s_1(\phi_1) \approx 5.45(10^3)\phi_1 - 0.004 \text{ [inches]} \tag{13a}$$

$$\Delta s_2(\phi_2) \approx 5.417(10^3)\phi_2 - 0.003 \text{ [inches]} \tag{13b}$$

$$\Delta s_3(\phi_3) \approx 5.426(10^3)\phi_3 - 0.004 \text{ [inches]} \tag{13c}$$

Equations (13a) through (13c) confirm the existence of a linear relationship between optical beam displacements and the shaft angle of twist. Although these equations can be used to calculate ϕ, the main idea has been to confirm linearity between shaft torsional displacements and the voltage response of the amplifier.

4.4.2. Determining ϕ and T from Amplifier Voltage Data

It was found that the voltage response of the amplifier varied linearly in proportion to the shaft angle of twist (i.e., through linear displacements of the reflected optical beam). As an initial standardization, it was necessary to correlate strain and voltage measurements. For the one, two, and three inch diameter shafts tested, respectively, the following inequalities relating γ to V_{Out} were realized:

$$0 \leq \gamma \leq 10(10^{-6})\ [\mu\varepsilon] \text{ constrained by: } 0 \leq V_{Out} \leq 11.2\ [\text{volts}] \tag{14a}$$

$$0 \leq \gamma \leq 20(10^{-6})\ [\mu\varepsilon] \text{ constrained by: } 0 \leq V_{Out} \leq 11.2\ [\text{volts}] \tag{14b}$$

$$0 \leq \gamma \leq 30(10^{-6})\ [\mu\varepsilon] \text{ constrained by: } 0 \leq V_{Out} \leq 11.2\ [\text{volts}] \tag{14c}$$

In each case, γ was used to calculate input torque to the shaft using equation (2); equation (4) was then used to compute ϕ. Using linear regression analysis, empirical equations relating amplifier voltage response as a function of ϕ were generated. For the one, two, and three inch shafts, the respective expressions are:

$$V_{Out}(\phi_1) = 1.879(10^5)\phi_1 - 0.274\ [\text{volts}] \tag{15a}$$

$$V_{Out}(\phi_2) = 1.912(10^5)\phi_2 - 0.374\ [\text{volts}] \tag{15b}$$

$$V_{Out}(\phi_3) = 1.9(10^5)\phi_3 - 0.24 \text{ [volts]} \quad (15c)$$

solving for ϕ_1, ϕ_2, and ϕ_3 yields:

$$\phi_1(V_{Out}) = 5.322(10^{-6})V_{Out} + 1.457(10^{-6}) \text{ [radians]} \quad (16a)$$

$$\phi_2(V_{Out}) = 5.229(10^{-6})V_{Out} + 1.953(10^{-6}) \text{ [radians]} \quad (16b)$$

$$\phi_3(V_{Out}) = 5.264(10^{-6})V_{Out} + 1.262(10^{-6}) \text{ [radians]} \quad (16c)$$

Substituting equations (16a), (16b), and (16c) into equation (4) and solving for shaft input torque yields:

$$T_1(V_{Out}) = \frac{GJ}{\Delta x}\left[5.322(10^{-6})V_{Out} + 1.457(10^{-6})\right] \quad (17a)$$

$$T_2(V_{Out}) = \frac{GJ}{\Delta x}\left[5.229(10^{-6})V_{Out} + 1.953(10^{-6})\right] \quad (17b)$$

$$T_3(V_{Out}) = \frac{GJ}{\Delta x}\left[5.264(10^{-6})V_{Out} + 1.262(10^{-6})\right] \quad (17c)$$

Equations (17a), (17b), and (17c) form to standardize input torque calculations to a 1045 or 4140 steel shaft based solely on optical dependent voltage measurements. Plots of these equations are shown in Figure 4.4.2.1 and illustrate the linearity of shaft input torque as a function of V_{Out}.

In order to demonstrate how close in accuracy V_{Out} compared for like values of ϕ amongst the three shafts tested, linear interpolation and error analysis was applied to equations (15a), (15b), and (15c). These results are tabulated in Table 4.5.1. A statistical analysis to determine experimental repeatability will follow.

$$T_1(V_1) := \frac{G \cdot J_1}{\Delta x} \cdot \left[5.322 \cdot 10^{-6} \cdot V_1 + 1.457 \cdot (10^{-6}) \right] \quad \text{(1" diameter shaft)}$$

$$T_2(V_2) := \frac{G \cdot J_2}{\Delta x} \cdot \left[5.229 \cdot 10^{-6} \cdot V_2 + 1.956 \cdot (10^{-6}) \right] \quad \text{(2" diameter shaft)}$$

$$T_3(V_3) := \frac{G \cdot J_3}{\Delta x} \cdot \left[5.264 \cdot 10^{-6} \cdot V_3 + 1.262 \cdot (10^{-6}) \right] \quad \text{(3" diameter shaft)}$$

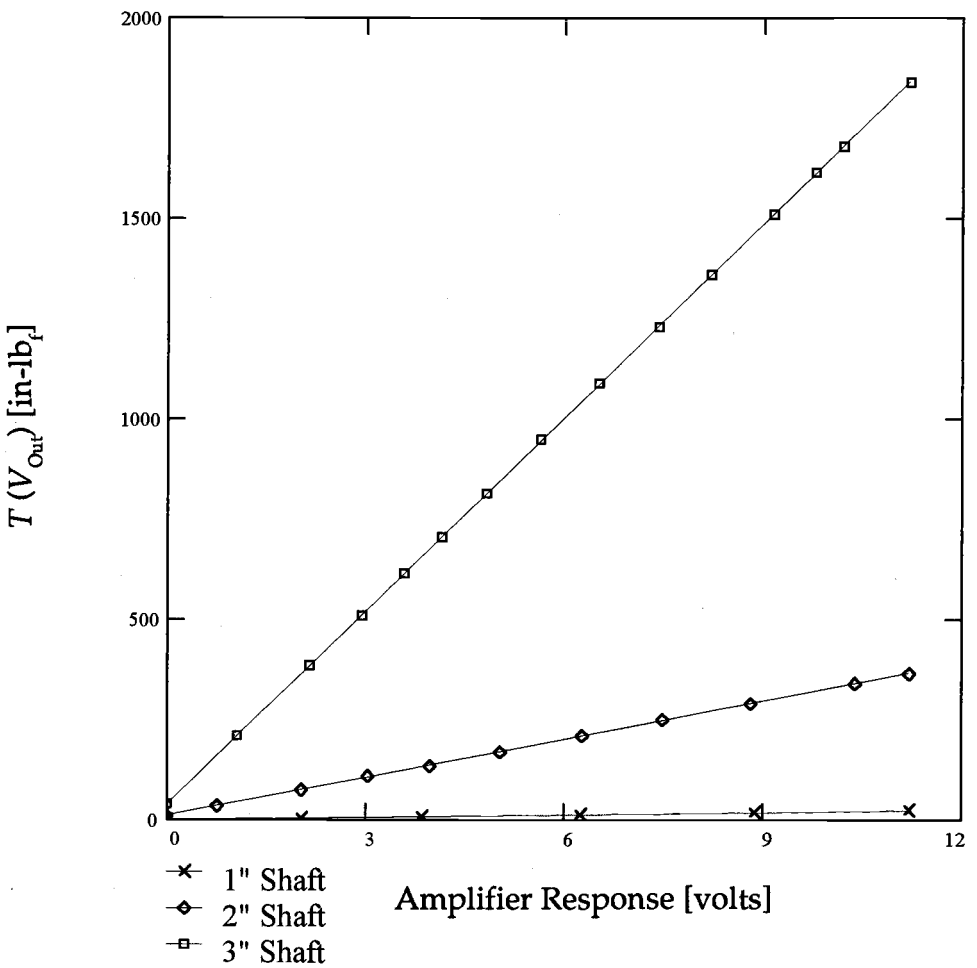

Figure 4.4.2.1. Linearized shaft input torque as a function of (V_{Out}).

4.5. Error and Statistical Analysis of Results

4.5.1. Error Analysis Performed on Voltage Data

Performing linear interpolation and error analysis on equations (15a), (15b), and (15c) for $0 \leq \phi \leq 6.0(10^{-5})$ radians yields the results in Table 4.5.1.1:

ϕ_{Range} (rads)	$V_1(\phi_{Range})$ (volts)	$V_2(\phi_{Range})$ (volts)	$V_3(\phi_{Range})$ (volts)	%Err(V_1,V_2)	%Err(V_1,V_3)	%Err(V_2,V_3)
0	0	0	0	0	0	0
$6.0(10^{-6})$	0.853	0.773	0.900	9.379	5.510	16.429
$8.0(10^{-6})$	1.229	1.156	1.280	5.940	4.150	10.727
$1.2(10^{-5})$	1.981	1.920	2.040	3.079	2.978	6.250
$1.6(10^{-5})$	2.732	2.685	2.800	1.717	2.484	4.283
$1.8(10^{-5})$	3.108	3.068	3.180	1.287	2.317	3.651
$2.0(10^{-5})$	3.484	3.450	3.560	0.976	2.181	3.188
$2.4(10^{-5})$	4.236	4.215	4.320	0.496	1.983	2.491
$2.8(10^{-5})$	4.987	4.980	5.080	0.140	1.865	2.008
$3.0(10^{-5})$	5.363	5.362	5.460	0.019	1.809	1.828
$3.2(10^{-5})$	5.739	5.744	5.840	0.087	1.760	1.671
$3.6(10^{-5})$	6.490	6.509	6.600	0.293	1.695	1.398
$4.0(10^{-5})$	7.242	7.274	7.360	0.442	1.629	1.182
$4.2(10^{-5})$	7.618	7.656	7.740	0.499	1.601	1.097
$4.4(10^{-5})$	7.994	8.039	8.120	0.563	1.576	1.008
$4.8(10^{-5})$	8.745	8.804	8.880	0.675	1.544	0.863
$5.2(10^{-5})$	9.479	9.568	9.640	0.939	1.696	0.753
$5.4(10^{-5})$	9.873	9.951	10.020	0.790	1.489	0.693
$5.6(10^{-5})$	10.248	10.333	10.400	0.829	1.483	0.648
$6.0(10^{-5})$	11.000	11.098	11.160	0.891	1.455	0.559

Table 4.5.1.1. Error analysis results of voltage data for all three shafts.

With respect to Table 4.5.1.1, it is apparent that as the shaft angle of twist was increased (i.e., a decrease in the amount of optical radiation absorbed by the CdS cell), the error between amplifier response voltages had a tendency to decrease. There are two probable causes for this phenomenon: (1) At lower voltage levels in the range of $0.733 \leq V_{Out} \leq 1.280$ V, it is speculated that low frequency band components (i.e., interference) were present at the amplifier output; or (2) high frequency band components (i.e., noise) were present at the amplifier output.

Inherently, no signal generated as a result of a voltage drop across the R_λ / R_3 resistive divider will be "pure". Contamination will always exist as a result of internal capacitance discharge, ripple, and other low band components generally categorized as interference. It is important to discern the difference between interference and noise in this context. Interference would be an error induced in the voltage drop across the R_λ / R_3 network; this is usually the result of parasitic circuit elements and cannot be predicted quantitatively. Though noise will also manifest itself as an error in a voltage measurement, its origin lies in the physical nature of the CdS device or the readout circuit; noise is a predictable performance parameter controlled by design.

Speculating that *interference* caused the errors tabulated in Table 4.4.1, then this problem could be minimized by placing a capacitor in parallel with the CdS device; this would cause any low band frequencies to pass through the capacitor and not through the terminals of the photoresistor. In addition, the DC voltage drops which make up the signal input to the noninverting terminal of the amplifier would be blocked by the capacitor.

Assuming that unwanted high band frequencies mixed with information containing signals in the readout circuitry, then a simple low-pass filter connected to the amplifier output would act to modulate any noise contaminated signals to ground (i.e., the capacitor would act as a short at these higher frequencies).

4.5.2. Statistical Analysis: Confirming Experimental Repeatability

With respect to measures of central tendency, all sets of observed voltage data had a distinct inclination to cluster about a central point. Thus for each of these data sets, it was reasonable to calculate an arithmetic mean voltage. For the one, two, and three inch shafts tested, this arithmetic mean voltage was used as a basis in deriving equations (15a) through (15c), such that $V_{Avg} = V_{Out}$. These voltages are tabulated in Table 4.5.2.1 and in Appendix A.

For the one inch shaft, the worst case measure of dispersion (i.e., the greatest variation of all data sets) resulted in a variance of 0.02 V^2 and a standard deviation of σ = 0.139 V for a mean voltage of = 2.02 V. Calculating plus-and-minus two standard deviations from the mean resulted in $+2\sigma$ = 2.298 V and -2σ = 1.742 V. At higher voltage levels, the standard deviation was at worst 95.1% of the mean and 99.8% at best.

For the two inch shaft, the greatest measures of dispersion resulted in a variance of 0.819 V^2 and σ = 0.905 for V_{Avg} = 0.747. The second worst case observed was $\sigma^2 = 0.072\ V^2$ and $\sigma = 0.269\ V_{Avg}$ for = 10.35 V. At other voltage levels, the standard deviation was at worst 96.7% of the mean and 98.9% at best.

For the three inch shaft, σ_{Max} = 0.05 V and σ_{Min} = 0.069 V for mean voltages of V_{Avg} = 1.063 and 8.201 V, respectively. At other voltage levels, the standard deviation was at worst 95.8% of the mean and 98.9% at best.

It would not be practical nor an efficient use of time to generate a frequency distribution for each of the observed data sets. Simple measures of central tendency and dispersion have provided reasonable assurance of obtaining reproducible findings.

1" diam. shaft		2" diam. shaft		3" diam. shaft	
ϕ_1 (rads)	V_{Out} (volts)	ϕ_2 (rads)	V_{Out} (volts)	ϕ_3 (rads)	V_{Out} (volts)
0	0	0	0	0	0
$1.2(10^{-5})$	2.02	$6.0(10^{-6})$	0.747	$8.0(10^{-6})$	1.07
$2.4(10^{-5})$	3.86	$1.2(10^{-5})$	2.02	$1.2(10^{-5})$	2.16
$3.6(10^{-5})$	6.23	$1.8(10^{-5})$	3.04	$1.6(10^{-5})$	2.93
$4.8(10^{-5})$	8.87	$2.4(10^{-5})$	3.97	$2.0(10^{-5})$	3.58
$6.0(10^{-5})$	11.2	$3.0(10^{-5})$	5.04	$2.4(10^{-5})$	4.14
		$3.6(10^{-5})$	6.27	$2.8(10^{-5})$	4.82
		$4.2(10^{-5})$	7.49	$3.2(10^{-5})$	5.65
		$4.8(10^{-5})$	8.82	$3.6(10^{-5})$	6.53
		$5.4(10^{-5})$	10.4	$4.0(10^{-5})$	7.41
		$6.0(10^{-5})$	11.2	$4.4(10^{-5})$	8.20
				$4.8(10^{-5})$	9.14
				$5.2(10^{-5})$	9.80
				$5.6(10^{-5})$	10.2
				$6.0(10^{-5})$	11.2

Table 4.5.2.1. Arithmetic mean voltages for corresponding values of ϕ.

Chapter 5. Conclusions and Recommendations for Future Research

5.1. Conclusions

The primary objective of this research was to design and experimentally test an optoelectronic system capable of measuring angular displacements in a torsionally loaded shaft through noncontact means.

A laser was used as an "optical gauge" in measuring shaft angle of twist (ϕ) in one and two inch 1045 steel shafts, and a three inch 4140 steel shaft. All shaft specimens tested were solid and circular. It was of interest to measure ϕ over a three inch segment of shaft length. Doing so by optical means was made possible by affixing mirrors at either end of the three inch segment. These mirrors were oriented at angles of 45 and 135 degrees with respect to the shaft surface. Due to small imperfections in the surface of each mirror used, the reflected optical beam was nonuniform in shape and intensity. This problem was minimized by using a system of lenses which acted to magnify the beam in only one dimension.

In order to determine how linearly the reflected optical beam would displace in proportion to ϕ, a simple ruler was used to measure incremental displacements (Δs) for every $\gamma = 2\ \mu\varepsilon$ of input. Due to limitations of discernment in the human eye, it was approximated that for every value of $\phi = 6.0(10^{-6})$ radians, a displacement of $\Delta s = 0.032$ inches resulted for each shaft tested. It was determined that the displacement Δs for small angles of ϕ was linear with torque. The magnitude of this linearity increased with the length of the optical lever arm.

Through observance of the linearity of optical beam displacement, it was speculated that a photosensitive circuit would produce a corresponding linear set of output voltages depending on the amount of optical radiation received by the photoconductor. This led to the design of a optically configured differential amplifier which was used to indirectly measure ϕ through a DC voltage response.

For a known set of input shaft strains, voltage and strain measurements were simultaneously recorded. Using values of shear strain to compute shaft input torque and ϕ, linear regression was fitted to these results to obtain linear relationships between ϕ, γ, and T as a function of the amplifier voltage response. The effectiveness of the experimental apparatus and techniques in this research were determined through error analysis of empirical equations of the form $V_{Out} = V_{Out}(\phi)$. The repeatability of experimental findings were determined using statistical analysis through measures of central tendency and dispersion. It was concluded that the optical techniques and apparatus of this work are effective in measuring shaft angular displacements. Also, the results obtained were verified to be reproducible.

5.2. Recommendations for Future Research

The future tasks recommended for future research and development may be summarized as follows:

(1) Selecting a more efficient photoconductive device: The CdS cell used in all of the experimental work produced favorable results only when the laser light was displace along the photoconducting surface; in addition, the circular surface of the device had to be masked off into a triangular configuration to maximize linearity in the voltage response of the amplifier.

(2) With respect to a prudent choice of a photoconductive device, a single conduction band cell with a tapered triangular cross section appears to be a suitable option. This would still allow for continuous voltage measurements.

(3) Using a densely packed photodiode array is also an attractive choice, especially since some of these packages contain built in digital read-

especially since some of these packages contain built in digital read-out circuits. For those packages that lack the extra electronics, the circuitry developed in this research could be used to augment such a device.

(4) The mirrors used in all of the experiments were first surface mirrors, which are very vulnerable to abrasions. It is recommended that hard coated 45° diagonal mirrors be used (e.g., Edmund Scientific N30,876, with a 20 mm^2 mounting surface). These mirrors have an elliptically shaped surface on a right angle prism shaped substrate.

(5) Augment the CdS dependent amplifier with an A/D converter, thus allowing for digitization of the analog response signal. The digitized response could be further processed by a preprogrammed computer for the sole purpose of obtaining values of shaft input torque in real time.

Bibliography

Brown, David, and Hamilton III, E.P., 1984, *Electromechanical Energy Conversion*, Macmillan Publishing Co., pp. 12-51.

Calder, C.A., 1994, personal communication.

Cooper, W.D., and Helfrick, A.D., 1985, *Electronic Instrumentation and Measurement Techniques*, Prentice-Hall, pp. 110-141, 353-359.

Fiore, J.M., 1992, *Operational Amplifiers and Linear Integrated Circuits: Theory and Applications*, West Publishing Co., pp. 87-119, 126-155.

Hughes, T.J., 1993, "A Spin on Torque Measurement," *Mechanical Engineering Magazine*, Vol. 24, No. 1, pp. 33-35.

Kennedy, T.C., 1994, personal communication.

Lemaitre, J., and Chaboche, J.L., 1990, *Mechanics of Solid Materials*, Cambridge University Press, pp. 41-53.

Mooney, W.J., 1991, *Optoelectronic Devices and Principles*, Prentice Hall, pp. 210-242.

O'Shea, D.C., 1977, *An Introduction to Lasers and their Applications*, Addison-Wesley Publishing Co., pp.1-3, 5-23

Pallas-Areny, R., and Webster, J.G., 1991, *Sensors and Signal Conditioning*, John Wiley & Sons, pp. 41-72.

Palm III, W.J., 1983, *Modeling, Analysis, and Control of Dynamic Systems*. John WIley & Soncs, pp. 5-92, 117-144.

Pantell, R.H., and Puthoff, H.E., 1969, *Fundamentals of Quantum Electronics*, John WIley & Soncs, pp. 1-11, 101-121.

Plant, T.K., 1994, personal communication.

Rosenstark, S., 1986, *Feedback Amplifier Principles*, Macmillan Publishing Co., pp. 27-37, 80-92.

Timoshenko, S., and Young, D.H., 1962, *Elements of Strength of Materials*, D. Van Nostrand Co., pp. 70-91.

Ward, J.P., 1992, *Solid Mechanics*, Kluner Academic Publishers, pp. 162-181.

Wilson, J., and Hawkes, J.F.B., 1989, *Optoelectronics: An Introduction*, Prentice Hall, pp. 1-10, 216-242.

Yariv, A., 1985, *Optical Electronics*, Holt, Rinehart, and Wilson, pp. 148-187.

Appendices

Appendix A. Treatment of Laboratory Data

In this section, recorded shear strain data and arithmetic mean voltages are treated using linear regression analysis. All units are expressed in inches, pounds, and volts. Shaft input torques and corresponding values of shaft angle of twist are also calculated. MathCad™ was used in processing all of the results.

A1.1. Data Set No. 1: Shaft Parameters and Recorded Strain/Displacements.

1-inch diameter 1045 steel shaft.

$i := 0..5$ — *This is the number of recorded data points.*

$\Delta x := 3$ — *This is the spacing between shaft test planes P_1 and P_2 (i.e., where mirrors M_1 and M_2 are affixed); units are in* ***inches****.*

$E := 30 \cdot 10^6$ — *This is Young's modulus for steel; units are in* ***lbf / in²****.*

$\nu := 0.3$ — *Poisson's ratio for steel.*

$G := \frac{E}{2 \cdot (1 + \nu)}$ — *Shear modulus of elasticity; units are in* ***lbf / in²****.*

$r_1 := 0.5$ — *Shaft radius; units are in* ***inches****.*

$J_1 := \frac{\pi \cdot r_1^4}{2}$ — *Polar moment of inertia; units are in* ***in⁴****.*

Data Set No. 1 (Continued):

$$T(\gamma_1) := \frac{G \cdot J_1 \cdot \gamma_1}{r_1}$$

This is the equation for calculating shaft input torque from shear strain data; units are in ***lbf / in²****.*

$$\phi(T_1) := \frac{T_1 \cdot \Delta x}{G \cdot J_1}$$

This is the equation for calculating the shaft angle of twist from input torque $T(\gamma_1)$*; units are in* ***radians****.*

Shear Strain (Output) Amplifier Voltage (Output) Calculated Torque (Input)

$$\gamma_1 := \begin{bmatrix} 0 \\ 2 \cdot 10^{-6} \\ 4 \cdot 10^{-6} \\ 6 \cdot 10^{-6} \\ 8 \cdot 10^{-6} \\ 10 \cdot 10^{-6} \end{bmatrix} \qquad V_1 := \begin{bmatrix} 0 \\ 2.02 \\ 3.86 \\ 6.23 \\ 8.87 \\ 11.2 \end{bmatrix} \qquad T(\gamma_1) = \begin{bmatrix} 0 \\ 4.531 \\ 9.062 \\ 13.593 \\ 18.125 \\ 22.656 \end{bmatrix}$$

Data Set No. 1 (Continued):

Torque Matrix (Intput) Angle of Twist (Output) Linear Beam Displacement

$$T_1 := \begin{bmatrix} 0 \\ 4.531 \\ 9.062 \\ 13.593 \\ 18.125 \\ 22.656 \end{bmatrix} \qquad \phi_1 := \begin{bmatrix} 0 \\ 1.2 \cdot 10^{-5} \\ 2.4 \cdot 10^{-5} \\ 3.6 \cdot 10^{-5} \\ 4.8 \cdot 10^{-5} \\ 6 \cdot 10^{-5} \end{bmatrix} \qquad \Delta s_1 := \begin{bmatrix} 0 \\ 0.063 \\ 0.125 \\ 0.188 \\ 0.250 \\ 0.313 \end{bmatrix}$$

Perform linear regression analysis. The slope = slope(γ_1,V_1) returns a scalar: The slope of the least-squares regression line for the shear strain-amplifier voltage data points. Similarly, slope = slope(ϕ_1,V_1), slope(ϕ_1,Δs_1), and slope(T_1,V_1) will be computed.

The intercept = intercept(γ_1,V_1) returns a scalar: The y-intercept of the least squares regression line for the shear strain-amplifier voltage data points. Similarly, intercept = intercept(ϕ_1,V_1), intercept(ϕ_1,Δs_1), and intercept(T_1,V_1) will be computed.

Treatment of Data Set No. 1

$m_1 := \text{slope}(\gamma_1, V_1)$ Therefore: $m_1 = 1.127 \cdot 10^6$

$b_1 := \text{intercept}(\gamma_1, V_1)$ and: $b_1 = -0.274$

The empirical equation for amplifier output voltage as a function of shear strain yields:

$$V_{Out}(\gamma_1) = 1.127(10^6)\gamma_1 - 0.274 \text{ [volts]}$$

where the slope m_1 has units of volts per microstrain. Solving this equation for γ_1 yields:

$$\gamma_1(V_{Out}) = 8.873(10^{-7})V_{Out} + 2.429(10^{-7}) \text{ [με]}$$

As for the angle of twist (ϕ_1) and linear displacement of the reflected optical beam (Δs_1), a similar analysis gives:

$m'_1 := \text{slope}(\phi_1, V_1)$ Therefore: $m'_1 = 1.879 \cdot 10^5$

$b'_1 := \text{intercept}(\phi_1, V_1)$ and: $b'_1 = -0.274$

and:

Treatment of Data Set No. 1 (Continued):

$m''_1 := \text{slope}(\phi_1, \Delta s_1)$ Therefore: $m''_1 = 5.212 \cdot 10^3$

$b''_1 := \text{intercept}(\phi_1, \Delta s_1)$ and: $b''_1 = 1.429 \cdot 10^{-4}$

The resultant empirical equations for: (1) The shaft angle of twist; and (2) linear optical beam displacement yield, respectively:

$$\phi_1(V_{Out}) = 5.322(10^{-6})V_{Out} + 1.457(10^{-6}) \text{ [radians]}$$

and:

$$\Delta s_1(\phi_1) = 5.212(10^3)\phi_1 + 1.429(10^{-4}) \text{ [inches]}$$

An expression relating input torque as a function of amplifier voltage response yields:

$m'''_1 := \text{slope}(T_1, V_1)$ Therefore: $m'''_1 = 0.498$

$b'''_1 := \text{intercept}(T_1, V_1)$ and: $b'''_1 = -0.274$

Thus:

$$T_1(V_{Out}) = 2.01V_{Out} + 0.55 \text{ [in-lb}_f\text{]}$$

A1.4. Plotting the Experimental Data Using Linear Regression Analysis

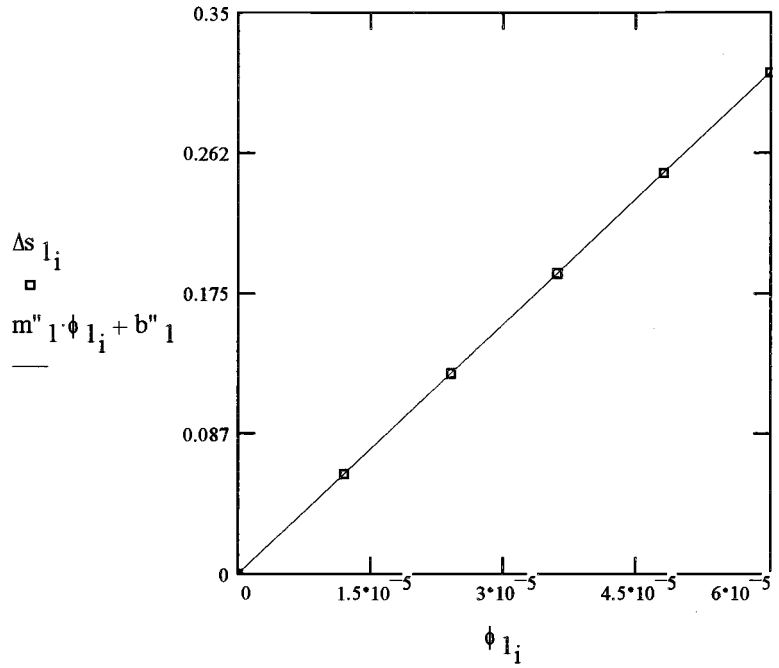

Figure A1.4.1a. Reflected optical beam displacement versus shaft angle of twist (1 inch diameter steel shaft).

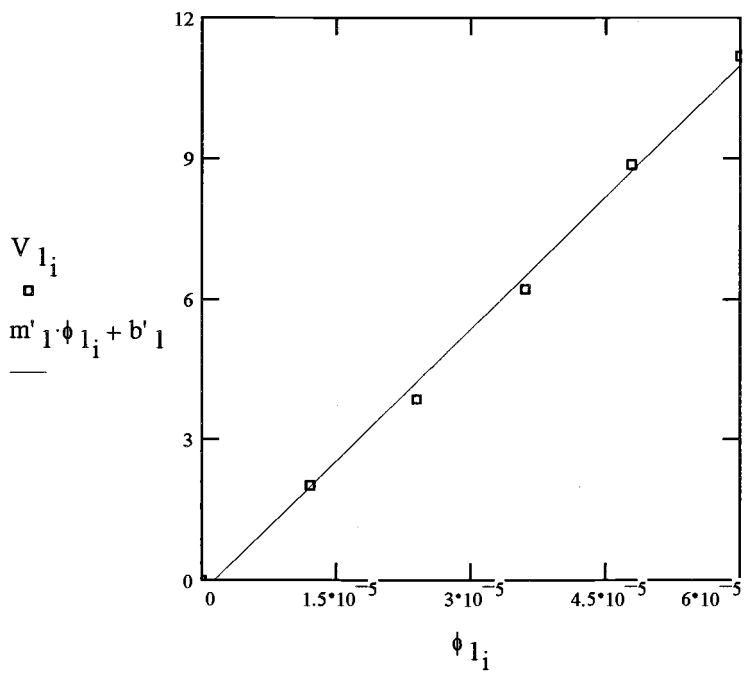

Figure A1.4.1b. Amplifier voltage response versus shaft angle of twist ϕ (1 inch diameter steel shaft).

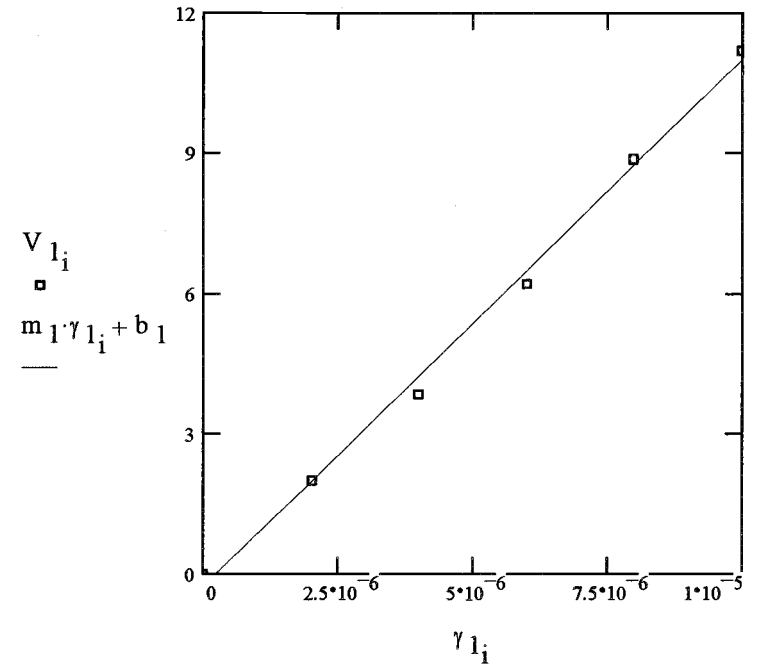

Figure A1.4.1c. Amplifier voltage response versus shaft shearing strain (1 inch diameter steel shaft).

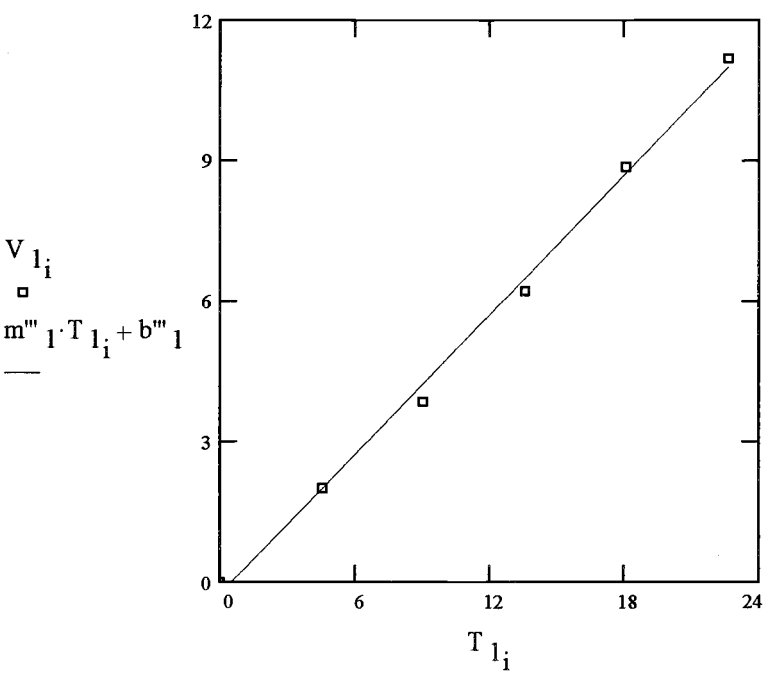

Figure A1.4.1d. Amplifier voltage response versus shaft input tprque (1 inch diameter steel shaft).

A1.2. Data Set No. 2: Shaft Parameters and Recorded Strain/Displacements.

2-inch diameter 1045 steel shaft.

$j := 0..10$ — *This is the number of recorded data points.*

$\Delta x := 3$ — *This is the spacing between shaft test planes P_1 and P_2 (i.e., where mirrors M_1 and M_2 are affixed); units are in* ***inches****.*

$E := 30 \cdot 10^6$ — *This is Young's modulus for steel; units are in* ***lbf / in²****.*

$\nu := 0.3$ — *Poisson's ratio for steel.*

$G := \frac{E}{2 \cdot (1 + \nu)}$ — *Shear modulus of elasticity; units are in* ***lbf / in²****.*

$r_2 := 1$ — *Shaft radius; units are in* ***inches****.*

$J_2 := \frac{\pi \cdot r_2^4}{2}$ — *Polar moment of inertia; units are in* ***in⁴****.*

Data Set No. 2 (Continued):

$$T(\gamma_2) := \frac{G \cdot J_2 \cdot \gamma_2}{r_2}$$

This is the equation for calculating shaft input torque from shear strain data; units are in ***lbf / in²****.*

$$\phi(T_2) := \frac{T_2 \cdot \Delta x}{G \cdot J_2}$$

This is the equation for calculating the shaft angle of twist from input torque $T(\gamma_2)$*; units are in* ***radians****.*

Shear Strain (Output) Amplifier Voltage (Output) Calculated Torque (Input)

$$\gamma_2 := \begin{bmatrix} 0 \\ 2 \cdot 10^{-6} \\ 4 \cdot 10^{-6} \\ 6 \cdot 10^{-6} \\ 8 \cdot 10^{-6} \\ 10 \cdot 10^{-6} \\ 12 \cdot 10^{-6} \\ 14 \cdot 10^{-6} \\ 16 \cdot 10^{-6} \\ 18 \cdot 10^{-6} \\ 20 \cdot 10^{-6} \end{bmatrix} \quad V_2 := \begin{bmatrix} 0 \\ 0.747 \\ 2.02 \\ 3.04 \\ 3.97 \\ 5.04 \\ 6.27 \\ 7.49 \\ 8.82 \\ 10.4 \\ 11.2 \end{bmatrix} \quad T(\gamma_2) = \begin{bmatrix} 0 \\ 36.249 \\ 72.498 \\ 108.747 \\ 144.997 \\ 181.246 \\ 217.495 \\ 253.744 \\ 289.993 \\ 326.242 \\ 362.491 \end{bmatrix}$$

Data Set No. 2 (Continued):

Torque Matrix (Intput) Angle of Twist (Output) Linear Beam Displacement

$$T_2 := \begin{bmatrix} 0 \\ 36.249 \\ 72.498 \\ 108.747 \\ 144.997 \\ 181.246 \\ 217.495 \\ 253.744 \\ 289.993 \\ 326.242 \\ 362.491 \end{bmatrix} \qquad \phi_2 := \begin{bmatrix} 0 \\ 6\cdot10^{-6} \\ 1.2\cdot10^{-5} \\ 1.8\cdot10^{-5} \\ 2.4\cdot10^{-5} \\ 3\cdot10^{-5} \\ 3.6\cdot10^{-5} \\ 4.2\cdot10^{-5} \\ 4.8\cdot10^{-5} \\ 5.4\cdot10^{-5} \\ 6\cdot10^{-5} \end{bmatrix} \qquad \Delta s_2 := \begin{bmatrix} 0 \\ 0.032 \\ 0.063 \\ 0.093 \\ 0.125 \\ 0.157 \\ 0.188 \\ 0.219 \\ 0.250 \\ 0.282 \\ 0.313 \end{bmatrix}$$

Perform linear regression analysis. The slope = slope(γ_2,V_2) returns a scalar: The slope of the least-squares regression line for the shear strain-amplifier voltage data points. Similarly, slope = slope(ϕ_2,V_2), slope(ϕ_2,Δs_2), and slope(T_2,V_2) will be computed.

The intercept = intercept(γ_2,V_2) returns a scalar: The y-intercept of the least squares regression line for the shear strain-amplifier voltage data points. Similarly, intercept = intercept(ϕ_2,V_2), intercept(ϕ_2,Δs_2), and intercept(T_2,V_2) will be computed.

Treatment of Data Set No. 2

$m_2 := \text{slope}(\gamma_2, V_2)$ Therefore: $m_2 = 5.737 \cdot 10^5$

$b_2 := \text{intercept}(\gamma_2, V_2)$ and: $b_2 = -0.374$

The empirical equation for amplifier output voltage as a function of shear strain yields:

$$V_{Out}(\gamma_2) = 5.737(10^5)\gamma_2 - 0.374 \text{ [volts]}$$

where the slope m_2 has units of volts per microstrain. Solving this equation for γ_2 yields:

$$\gamma_2(V_{Out}) = 1.743(10^{-6})V_{Out} + 6.511(10^{-7}) \text{ [}\mu\varepsilon\text{]}$$

As for the angle of twist (ϕ_2) and linear displacement of the reflected optical beam (Δs_2), a similar analysis gives:

$m'_2 := \text{slope}(\phi_2, V_2)$ Therefore: $m'_2 = 1.912 \cdot 10^5$

$b'_2 := \text{intercept}(\phi_2, V_2)$ and: $b'_2 = -0.374$

and:

Treatment of Data Set No. 2 (Continued):

$m''_2 := \text{slope}(\phi_2, \Delta s_2)$ Therefore: $m''_2 = 5.214 \cdot 10^3$

$b''_2 := \text{intercept}(\phi_2, \Delta s_2)$ and: $b''_2 = 1.364 \cdot 10^{-4}$

The resultant empirical equations for: (1) The shaft angle of twist; and (2) linear optical beam displacement yield, respectively:

$$\phi_2(V_{Out}) = 5.229(10^{-6})V_{Out} + 1.953(10^{-6}) \text{ [radians]}$$

and:

$$\Delta s_2(\phi_2) = 5.214(10^3)\phi_2 + 1.364(10^{-4}) \text{ [inches]}$$

An expression relating input torque as a function of amplifier voltage response yields:

$m'''_2 := \text{slope}(T_2, V_2)$ Therefore: $m'''_2 = 0.032$

$b'''_2 := \text{intercept}(T_2, V_2)$ and: $b'''_2 = -0.374$

Thus:

$$T_2(V_{Out}) = 31.593V_{Out} + 11.801 \text{ [in-lb}_f\text{]}$$

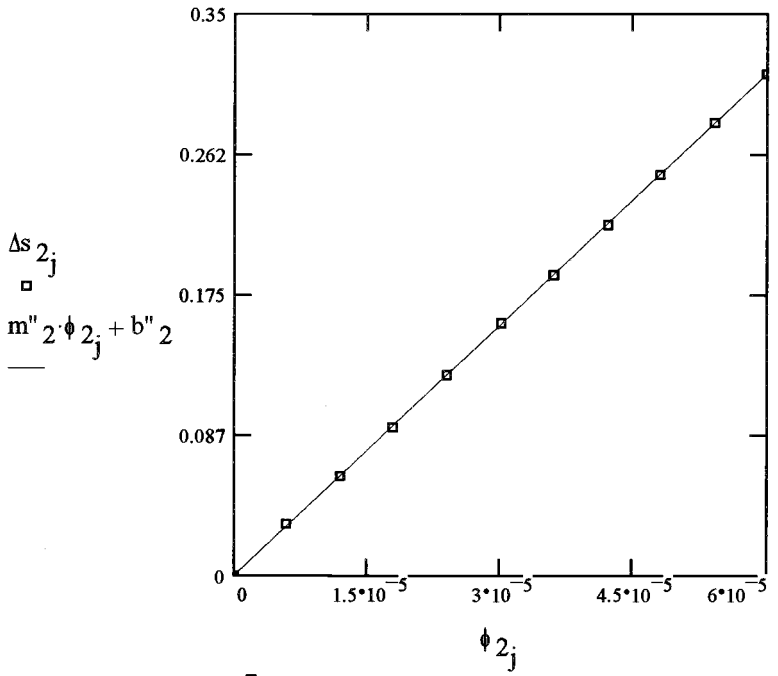

Figure A1.4.1e. Reflected optical beam displacement versus shaft angle of twist (2 inch diameter steel shaft).

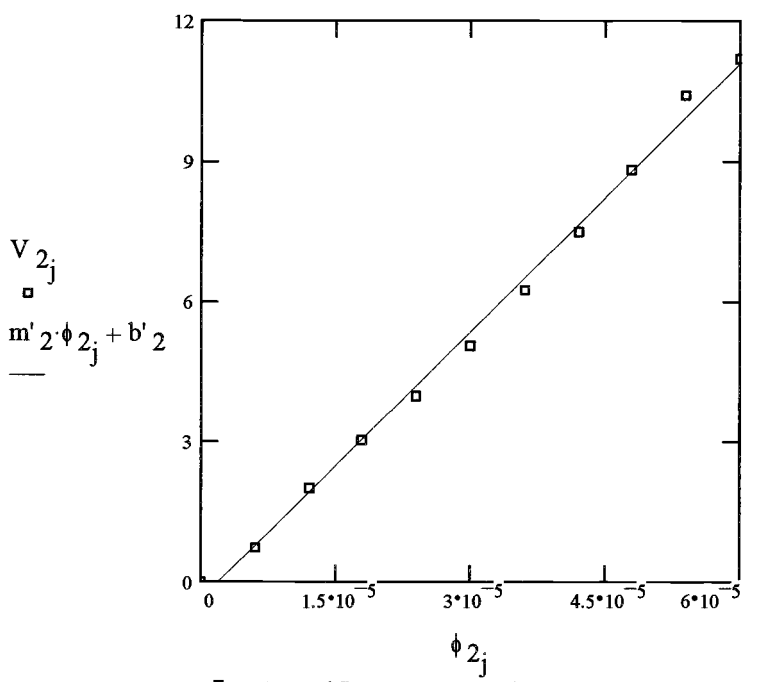

Figure A1.4.1f. Amplifier voltage response versus shaft angle of twist ϕ (2 inch diameter steel shaft).

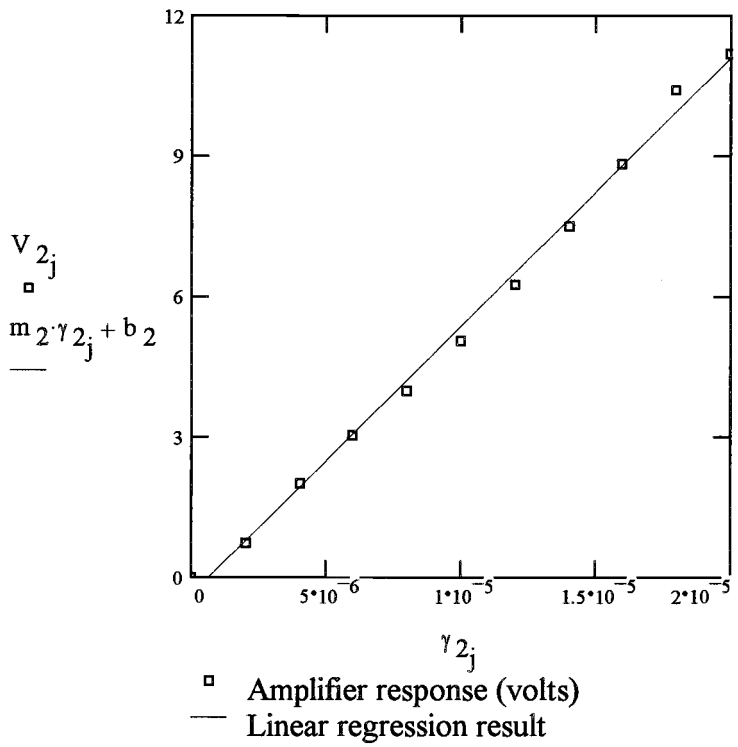

Figure A1.4.1g. Amplifier voltage response versus shaft shearing strain (2 inch diameter steel shaft).

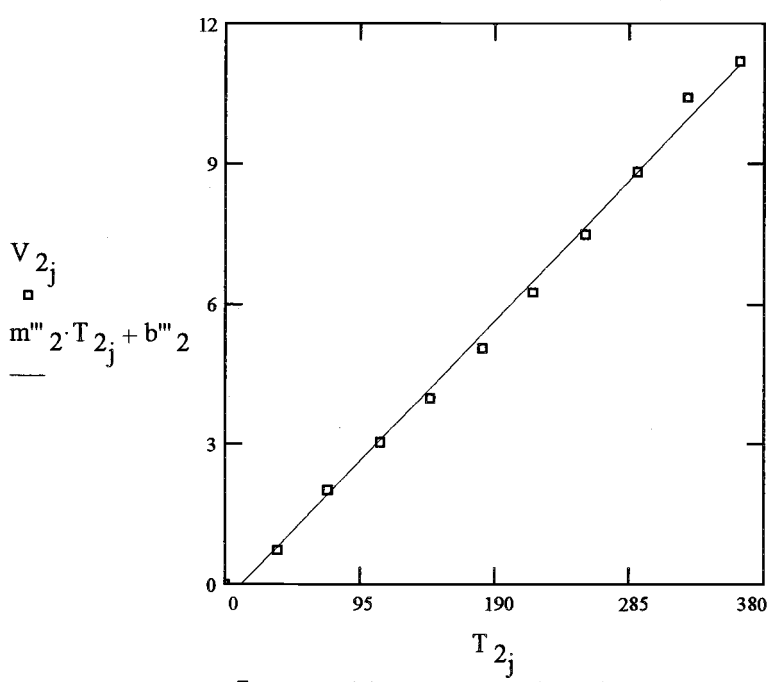

Figure A1.4.1h. Amplifier voltage response versus shaft input torque (2 inch diameter steel shaft).

A1.3. Data Set No. 3: Shaft Parameters and Recorded Strain/Displacements.

3-inch diameter 4140 steel shaft.

$k := 0 .. 14$ — *This is the number of recorded data points.*

$\Delta x := 3$ — *This is the spacing between shaft test planes P_1 and P_2 (i.e., where mirrors M_1 and M_2 are affixed); units are in* ***inches****.*

$E := 30 \cdot 10^6$ — *This is Young's modulus for steel; units are in* ***lbf / in²****.*

$\nu := 0.3$ — *Poisson's ratio for steel.*

$G := \frac{E}{2 \cdot (1 + \nu)}$ — *Shear modulus of elasticity; units are in* ***lbf / in²****.*

$r_3 := 1.5$ — *Shaft radius; units are in* ***inches****.*

$J_3 := \frac{\pi \cdot r_3^4}{2}$ — *Polar moment of inertia; units are in* ***in⁴****.*

Data Set No. 3 (Continued):

$$T(\gamma_3) := \frac{G \cdot J_3 \cdot \gamma_3}{r_3}$$

This is the equation for calculating shaft input torque from shear strain data; units are in ***lbf / in²****.*

$$\phi(T_3) := \frac{T_3 \cdot \Delta x}{G \cdot J_3}$$

This is the equation for calculating the shaft angle of twist from input torque $T(\gamma_3)$*; units are in* ***radians****.*

Shear Strain (Output) Amplifier Voltage (Output) Calculated Torque (Input)

$$\gamma_3 := \begin{bmatrix} 0 \\ 4\cdot10^{-6} \\ 6\cdot10^{-6} \\ 8\cdot10^{-6} \\ 10\cdot10^{-6} \\ 12\cdot10^{-6} \\ 14\cdot10^{-6} \\ 16\cdot10^{-6} \\ 18\cdot10^{-6} \\ 20\cdot10^{-6} \\ 22\cdot10^{-6} \\ 24\cdot10^{-6} \\ 26\cdot10^{-6} \\ 28\cdot10^{-6} \\ 30\cdot10^{-6} \end{bmatrix} \qquad V_3 := \begin{bmatrix} 0 \\ 1.07 \\ 2.16 \\ 2.93 \\ 3.58 \\ 4.14 \\ 4.82 \\ 5.65 \\ 6.53 \\ 7.41 \\ 8.20 \\ 9.14 \\ 9.8 \\ 10.2 \\ 11.2 \end{bmatrix} \qquad T(\gamma_3) = \begin{bmatrix} 0 \\ 244.682 \\ 367.023 \\ 489.363 \\ 611.704 \\ 734.045 \\ 856.386 \\ 978.727 \\ 1.101\cdot10^{3} \\ 1.223\cdot10^{3} \\ 1.346\cdot10^{3} \\ 1.468\cdot10^{3} \\ 1.59\cdot10^{3} \\ 1.713\cdot10^{3} \\ 1.835\cdot10^{3} \end{bmatrix}$$

Data Set No. 3 (Continued):

Torque Matrix (Intput) Angle of Twist (Output) Linear Beam Displacement

$$T_3 := \begin{bmatrix} 0 \\ 244.682 \\ 367.023 \\ 489.363 \\ 611.704 \\ 734.045 \\ 856.386 \\ 978.727 \\ 1.101 \cdot 10^3 \\ 1.223 \cdot 10^3 \\ 1.346 \cdot 10^3 \\ 1.468 \cdot 10^3 \\ 1.59 \cdot 10^3 \\ 1.713 \cdot 10^3 \\ 1.835 \cdot 10^3 \end{bmatrix} \qquad \phi_3 := \begin{bmatrix} 0 \\ 8 \cdot 10^{-6} \\ 1.2 \cdot 10^{-5} \\ 1.6 \cdot 10^{-5} \\ 2 \cdot 10^{-5} \\ 2.4 \cdot 10^{-5} \\ 2.8 \cdot 10^{-5} \\ 3.2 \cdot 10^{-5} \\ 3.6 \cdot 10^{-5} \\ 3.999 \cdot 10^{-5} \\ 4.401 \cdot 10^{-5} \\ 4.8 \cdot 10^{-5} \\ 5.199 \cdot 10^{-5} \\ 5.601 \cdot 10^{-5} \\ 6 \cdot 10^{-5} \end{bmatrix} \qquad \Delta s_3 := \begin{bmatrix} 0 \\ 0.042 \\ 0.063 \\ 0.083 \\ 0.104 \\ 0.125 \\ 0.146 \\ 0.167 \\ 0.188 \\ 0.208 \\ 0.229 \\ 0.250 \\ 0.271 \\ 0.292 \\ 0.313 \end{bmatrix}$$

Perform linear regression analysis. The slope = slope(γ_3,V_3) returns a scalar: The slope of the least-squares regression line for the shear strain-amplifier voltage data points. Similarly, slope = slope(ϕ_3,V_3), slope(ϕ_3,Δs_3), and slope(T_3,V_3) will be computed.

The intercept = intercept(γ_3,V_3) returns a scalar: The y-intercept of the least squares regression line for the shear strain-amplifier voltage data points. Similarly, intercept = intercept(ϕ_3,V_3), intercept(ϕ_3,Δs_3), and intercept(T_3,V_3) will be computed.

Treatment of Data Set No. 3

$m_3 := \text{slope}(\gamma_3, V_3)$ Therefore: $m_3 = 3.799 \cdot 10^5$

$b_3 := \text{intercept}(\gamma_3, V_3)$ and: $b_3 = -0.24$

The empirical equation for amplifier output voltage as a function of shear strain yields:

$$V_{Out}(\gamma_3) = 3.799(10^5)\gamma_3 - 0.24 \text{ [volts]}$$

where the slope m_3 has units of volts per microstrain. Solving this equation for γ_3 yields:

$$\gamma_3(V_{Out}) = 2.632(10^{-6})V_{Out} + 6.312(10^{-7}) \text{ [με]}$$

As for the angle of twist (ϕ_3) and linear displacement of the reflected optical beam (Δs_3), a similar analysis gives:

$m'_3 := \text{slope}(\phi_3, V_3)$ Therefore: $m'_3 = 1.9 \cdot 10^5$

$b'_3 := \text{intercept}(\phi_3, V_3)$ and: $b'_3 = -0.24$

and:

Treatment of Data Set No. 3 (Continued):

$m''_3 := \text{slope}(\phi_3, \Delta s_3)$ Therefore: $m''_3 = 5.211 \cdot 10^3$

$b''_3 := \text{intercept}(\phi_3, \Delta s_3)$ and: $b''_3 = 4.552 \cdot 10^{-5}$

The resultant empirical equations for: (1) The shaft angle of twist; and (2) linear optical beam displacement yield, respectively:

$$\phi_3(V_{Out}) = 5.264(10^{-6})V_{Out} + 1.262(10^{-6}) \text{ [radians]}$$

and:

$$\Delta s_3(\phi_3) = 5.211(10^3)\phi_3 + 4.552(10^{-5}) \text{ [inches]}$$

An expression relating input torque as a function of amplifier voltage response yields:

$m'''_3 := \text{slope}(T_3, V_3)$ Therefore: $m'''_3 = 0.006$

$b'''_3 := \text{intercept}(T_3, V_3)$ and: $b'''_3 = -0.24$

Thus:

$$T_3(V_{Out}) = 160.988V_{Out} + 38.621 \text{ [in-lb}_f\text{]}$$

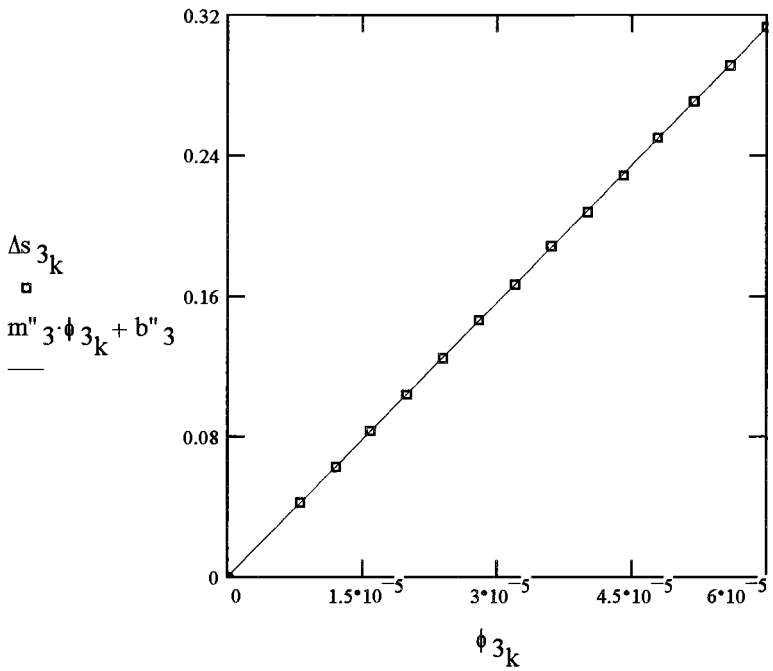

Figure A1.4.1i. Reflected opical beam displacement versus shaft angle of twist (3 inch diameter steel shaft).

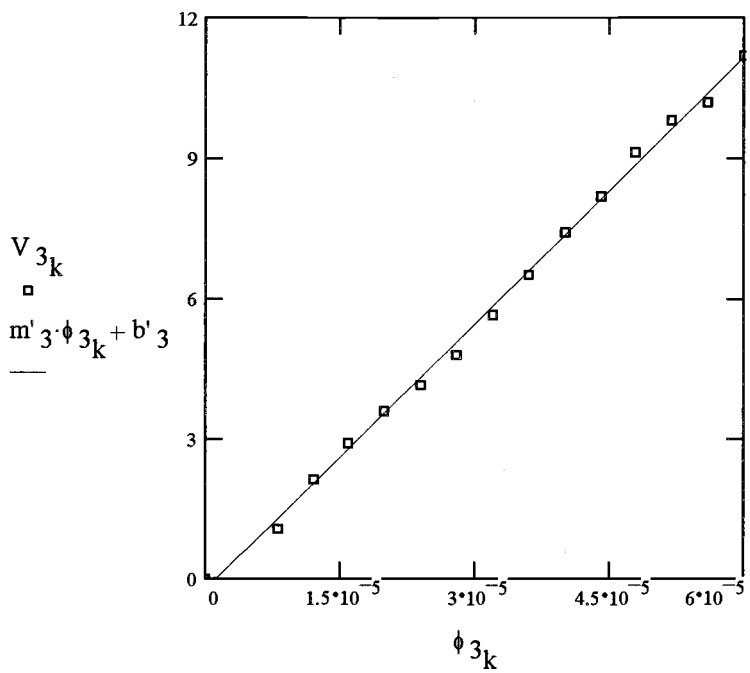

Figure A1.4.1j. Amplifier voltage response versus shaft angle of twist ϕ (3 inch diameter steel shaft).

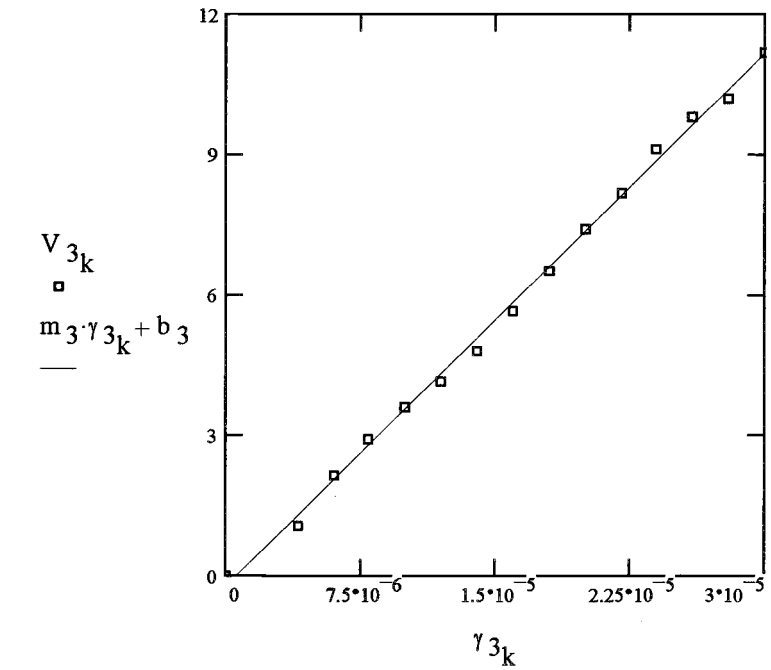

Figure A1.4.1k. Amplifier voltage response versus shaft shearing strain (3 inch diameter steel shaft).

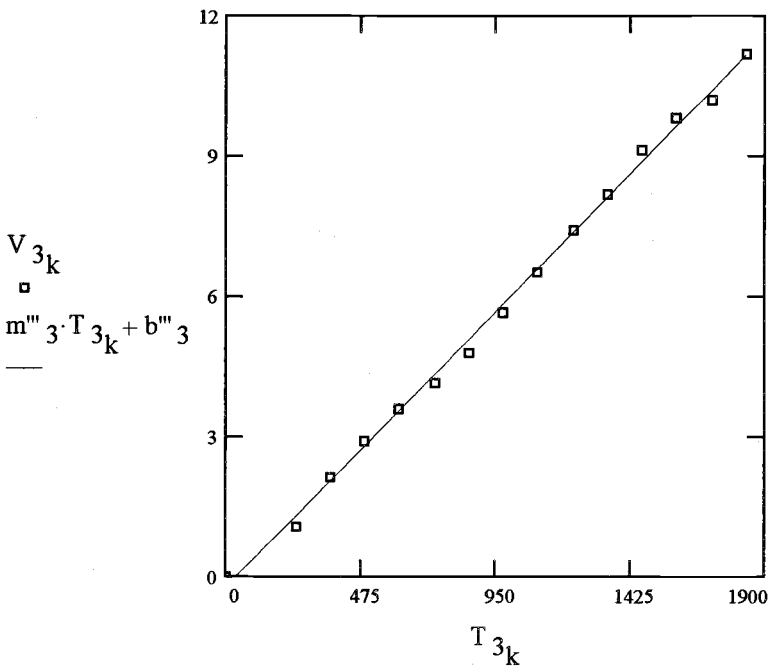

Figure A1.4.1l. Amplifier voltage response versus shaft input torque (3 inch diameter steel shaft).

$$\Delta s_1(\phi_1) := 5.212 \cdot 10^3 \cdot \phi_1 + 1.429 \cdot 10^{-4}$$

$$\Delta s_2(\phi_2) := 5.214 \cdot 10^3 \cdot \phi_2 + 1.364 \cdot 10^{-4}$$

$$\Delta s_3(\phi_3) := 5.211 \cdot 10^3 \cdot \phi_3 + 4.552 \cdot 10^{-5}$$

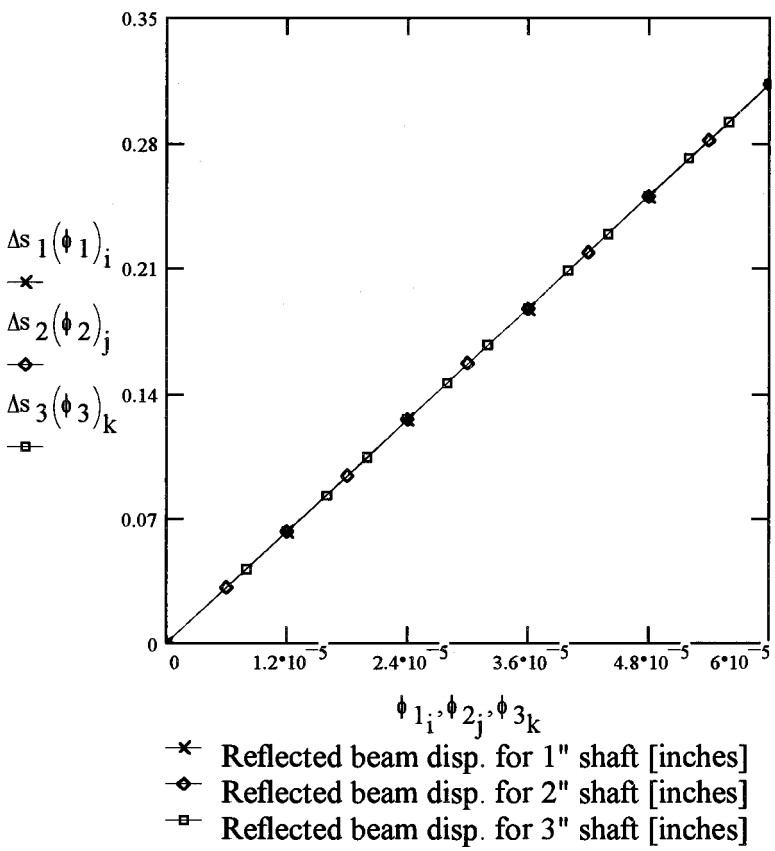

Figure A1.4.1m. Reflected laser beam displacement (Δs) versus shaft angle of twist (ϕ).

$$V_1(\phi_1) := 1.879 \cdot 10^5 \cdot \phi_1 - 0.274$$

$$V_2(\phi_2) := 1.912 \cdot 10^5 \cdot \phi_2 - 0.374$$

$$V_3(\phi_3) := 1.9 \cdot 10^5 \cdot \phi_3 - 0.24$$

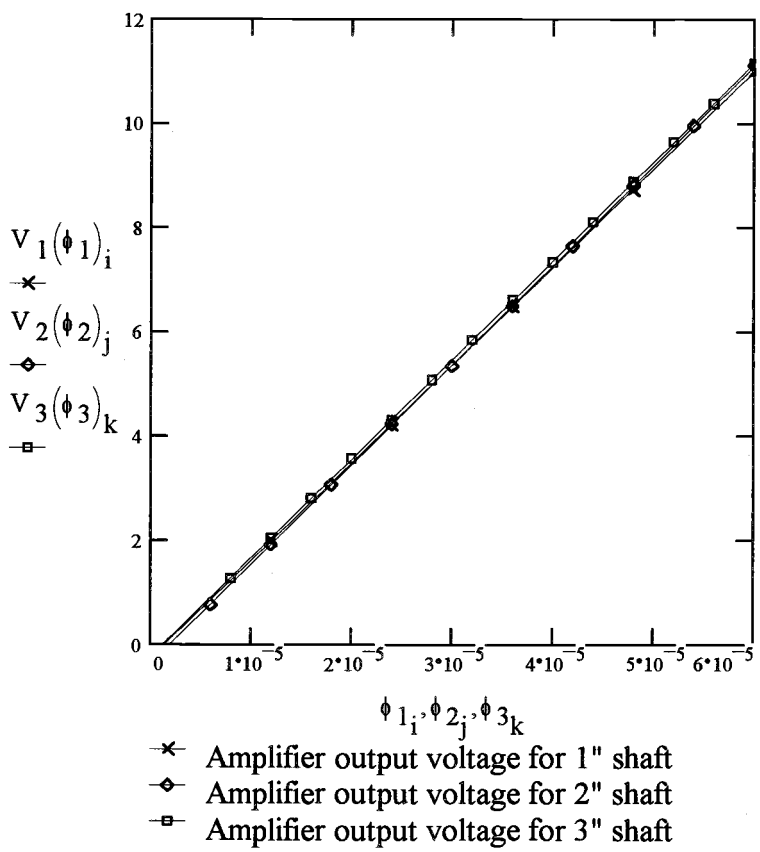

Figure A1.4.1n. Amplifier output voltage (V) versus shaft angle of twist (ϕ).

$$V_1(\gamma_1) := 1.127 \cdot 10^6 \cdot \gamma_1 - 0.274$$

$$V_2(\gamma_2) := 5.737 \cdot 10^5 \cdot \gamma_2 - 0.374$$

$$V_3(\gamma_3) := 3.799 \cdot 10^5 \cdot \gamma_3 - 0.24$$

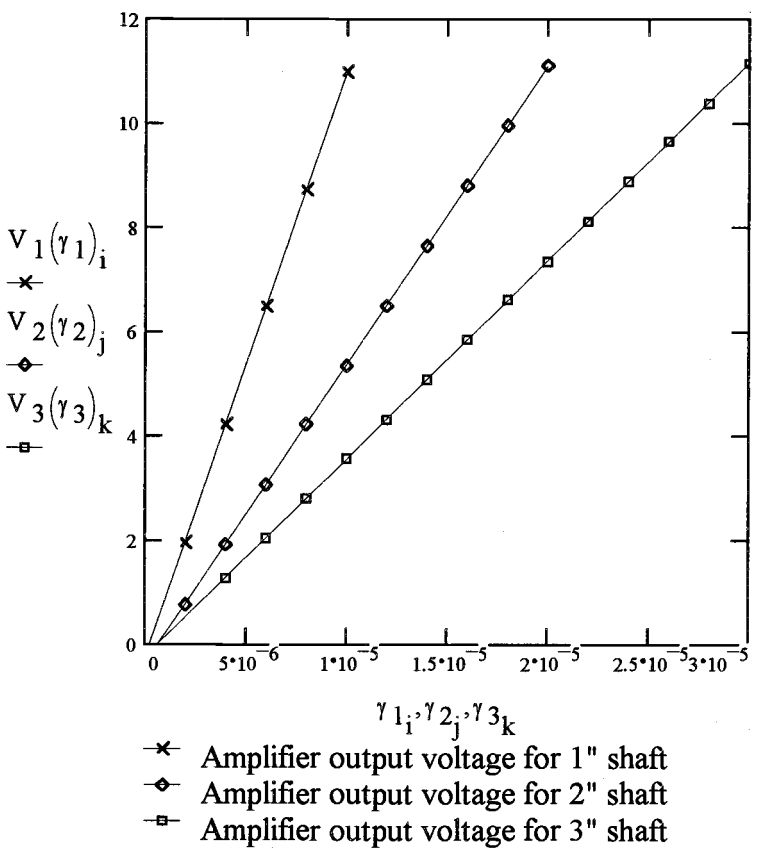

Figure A1.4.1o. Amplifier output voltage (V) versus shaft shearing strain (γ).

$$V_1(T_1) := 0.498 \cdot T_1 - 0.274$$

$$V_2(T_2) := 0.032 \cdot T_2 - 0.374$$

$$V_3(T_3) := 0.006 \cdot T_3 - 0.24$$

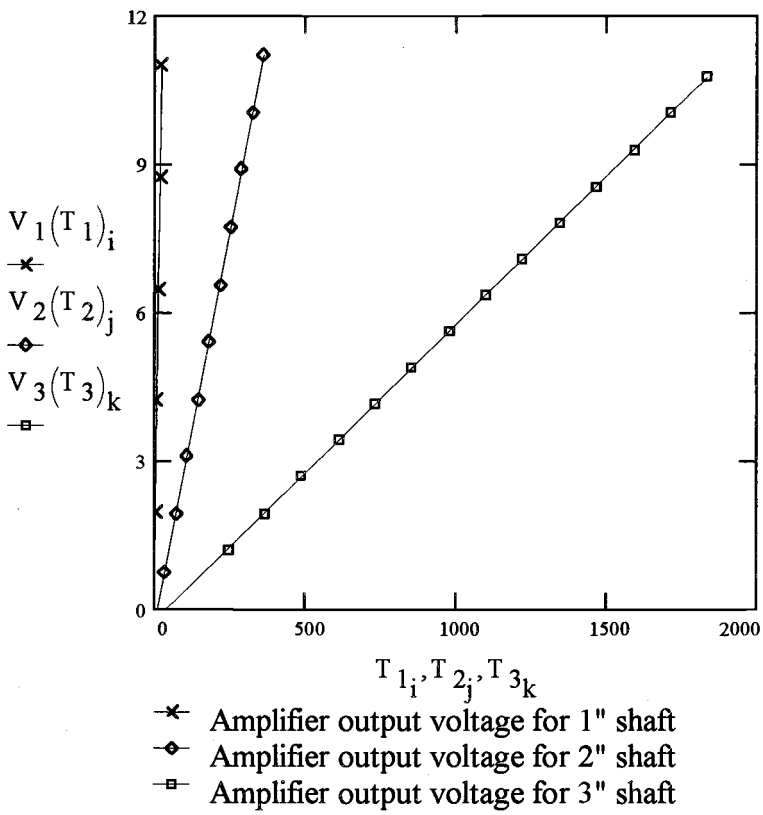

Figure A1.4.1p. Amplifier output voltage (V) versus shaft input torque (T).

Appendix B. Statistical Analysis of Amplifier Voltage Response To Estimate Experimental Repeatability

In this section, MathCad was used to perform a statistical analysis on raw voltage measurements. For each shaft tested, eight experiments were performed in order to assure experimental repeatability.

For consistently repeated values of input strain, corresponding values of amplifier output voltage were recorded; these discretized voltage sets have been labeled Data Set A, B, C, etc. Experimental repeatability has been determined through measures of central tendency and dispersion on each of these data sets.

B1.1. Statistical Analysis of Amplifier Voltage Response Data To Estimate Experimental Repeatability

1-inch diameter 1045 steel shaft.

$i := 0..7$

$$\text{Data}_A \equiv \begin{bmatrix} 1.97 \\ 1.74 \\ 2.12 \\ 2.07 \\ 2.14 \\ 2.21 \\ 1.99 \\ 1.92 \end{bmatrix}$$

$\text{mean}(\text{Data}_A) = 2.02$

$\text{stdev}(\text{Data}_A) = 0.139$

$\text{plus2sig} := \text{mean}(\text{Data}_A) + 2 \cdot \text{stdev}(\text{Data}_A)$

$\text{plus2sig} = 2.298$

$\text{minus2sig} := \text{mean}(\text{Data}_A) - 2 \cdot \text{stdev}(\text{Data}_A)$

$\text{minus2sig} = 1.742$

$$\text{Data}_B \equiv \begin{bmatrix} 3.72 \\ 3.67 \\ 4.11 \\ 4.02 \\ 3.87 \\ 3.52 \\ 3.92 \\ 4.03 \end{bmatrix}$$

$\text{mean}(\text{Data}_B) = 3.857$

$\text{stdev}(\text{Data}_B) = 0.191$

$\text{plus2sig} := \text{mean}(\text{Data}_B) + 2 \cdot \text{stdev}(\text{Data}_B)$

$\text{plus2sig} = 4.24$

$\text{minus2sig} := \text{mean}(\text{Data}_B) - 2 \cdot \text{stdev}(\text{Data}_B)$

$\text{minus2sig} = 3.475$

$$\text{Data}_C \equiv \begin{bmatrix} 6.52 \\ 6.07 \\ 6.34 \\ 6.13 \\ 5.98 \\ 6.41 \\ 6.29 \\ 6.13 \end{bmatrix}$$

$\text{mean}(\text{Data}_C) = 6.234$

$\text{stdev}(\text{Data}_C) = 0.173$

$\text{plus2sig} := \text{mean}(\text{Data}_C) + 2 \cdot \text{stdev}(\text{Data}_C)$

$\text{plus2sig} = 6.58$

$\text{minus2sig} := \text{mean}(\text{Data}_C) - 2 \cdot \text{stdev}(\text{Data}_C)$

$\text{minus2sig} = 5.887$

$$\text{Data}_D \equiv \begin{bmatrix} 8.92 \\ 8.72 \\ 8.94 \\ 8.83 \\ 8.79 \\ 9.02 \\ 8.81 \\ 8.87 \end{bmatrix}$$

$\text{mean}(\text{Data}_D) = 8.863$

$\text{stdev}(\text{Data}_D) = 0.089$

$\text{plus2sig} := \text{mean}(\text{Data}_D) + 2 \cdot \text{stdev}(\text{Data}_D)$

$\text{plus2sig} = 9.041$

$\text{minus2sig} := \text{mean}(\text{Data}_D) - 2 \cdot \text{stdev}(\text{Data}_D)$

$\text{minus2sig} = 8.684$

B1.2. Statistical Analysis of Amplifier Voltage Response Data To Estimate Experimental Repeatability

2-inch diameter 1045 steel shaft.

$i := 0..7$

$$\text{Data}_A \equiv \begin{bmatrix} 0.582 \\ 0.709 \\ 0.727 \\ 0.782 \\ 0.749 \\ 0.767 \\ 0.778 \\ 0.882 \end{bmatrix}$$

$\text{mean}(\text{Data}_A) = 0.747$

$\text{stdev}(\text{Data}_A) = 0.079$

$\text{plus2sig} := \text{mean}(\text{Data}_A) + 2 \cdot \text{stdev}(\text{Data}_A)$

$\text{plus2sig} = 0.905$

$\text{minus2sig} := \text{mean}(\text{Data}_A) - 2 \cdot \text{stdev}(\text{Data}_A)$

$\text{minus2sig} = 0.589$

$$\text{Data}_B \equiv \begin{bmatrix} 1.97 \\ 2.05 \\ 2.11 \\ 2.06 \\ 2.02 \\ 1.96 \\ 2.12 \\ 1.92 \end{bmatrix}$$

$\text{mean}(\text{Data}_B) = 2.026$

$\text{stdev}(\text{Data}_B) = 0.067$

$\text{plus2sig} := \text{mean}(\text{Data}_B) + 2 \cdot \text{stdev}(\text{Data}_B)$

$\text{plus2sig} = 2.161$

$\text{minus2sig} := \text{mean}(\text{Data}_B) - 2 \cdot \text{stdev}(\text{Data}_B)$

$\text{minus2sig} = 1.891$

$$\text{Data}_C \equiv \begin{bmatrix} 3.03 \\ 3.07 \\ 2.98 \\ 3.12 \\ 3.08 \\ 2.96 \\ 3.04 \\ 3.02 \end{bmatrix}$$

$\text{mean}(\text{Data}_C) = 3.037$

$\text{stdev}(\text{Data}_C) = 0.049$

$\text{plus2sig} := \text{mean}(\text{Data}_C) + 2 \cdot \text{stdev}(\text{Data}_C)$

$\text{plus2sig} = 3.136$

$\text{minus2sig} := \text{mean}(\text{Data}_C) - 2 \cdot \text{stdev}(\text{Data}_C)$

$\text{minus2sig} = 2.939$

$$\text{Data}_D \equiv \begin{bmatrix} 3.82 \\ 4.05 \\ 3.96 \\ 4.11 \\ 4.02 \\ 3.88 \\ 4.02 \\ 3.96 \end{bmatrix}$$

$\text{mean}(\text{Data}_D) = 3.977$

$\text{stdev}(\text{Data}_D) = 0.088$

$\text{plus2sig} := \text{mean}(\text{Data}_D) + 2 \cdot \text{stdev}(\text{Data}_D)$

$\text{plus2sig} = 4.153$

$\text{minus2sig} := \text{mean}(\text{Data}_D) - 2 \cdot \text{stdev}(\text{Data}_D)$

$\text{minus2sig} = 3.802$

$$\text{Data}_E \equiv \begin{bmatrix} 5.04 \\ 5.07 \\ 4.98 \\ 5.05 \\ 5.12 \\ 5.01 \\ 5.14 \\ 4.88 \end{bmatrix}$$

$\text{mean}(\text{Data}_E) = 5.036$

$\text{stdev}(\text{Data}_E) = 0.077$

$\text{plus2sig} := \text{mean}(\text{Data}_E) + 2 \cdot \text{stdev}(\text{Data}_E)$

$\text{plus2sig} = 5.19$

$\text{minus2sig} := \text{mean}(\text{Data}_E) - 2 \cdot \text{stdev}(\text{Data}_E)$

$\text{minus2sig} = 4.882$

$$\text{Data}_F \equiv \begin{bmatrix} 6.38 \\ 6.22 \\ 6.12 \\ 6.27 \\ 6.42 \\ 6.23 \\ 6.19 \\ 6.29 \end{bmatrix}$$

$\text{mean}(\text{Data}_F) = 6.265$

$\text{stdev}(\text{Data}_F) = 0.092$

$\text{plus2sig} := \text{mean}(\text{Data}_F) + 2 \cdot \text{stdev}(\text{Data}_F)$

$\text{plus2sig} = 6.449$

$\text{minus2sig} := \text{mean}(\text{Data}_F) - 2 \cdot \text{stdev}(\text{Data}_F)$

$\text{minus2sig} = 6.081$

$$\text{Data}_G \equiv \begin{bmatrix} 7.52 \\ 7.61 \\ 7.43 \\ 7.39 \\ 7.47 \\ 7.41 \\ 7.63 \\ 7.44 \end{bmatrix}$$

$\text{mean}(\text{Data}_G) = 7.487$

$\text{stdev}(\text{Data}_G) = 0.085$

$\text{plus2sig} := \text{mean}(\text{Data}_G) + 2 \cdot \text{stdev}(\text{Data}_G)$

$\text{plus2sig} = 7.657$

$\text{minus2sig} := \text{mean}(\text{Data}_G) - 2 \cdot \text{stdev}(\text{Data}_G)$

$\text{minus2sig} = 7.318$

$$\text{Data}_H \equiv \begin{bmatrix} 10.7 \\ 9.98 \\ 10.6 \\ 10.3 \\ 9.92 \\ 10.4 \\ 10.3 \\ 10.6 \end{bmatrix}$$

$\text{mean}(\text{Data}_H) = 10.35$

$\text{stdev}(\text{Data}_H) = 0.269$

$\text{plus2sig} := \text{mean}(\text{Data}_H) + 2 \cdot \text{stdev}(\text{Data}_H)$

$\text{plus2sig} = 10.887$

$\text{minus2sig} := \text{mean}(\text{Data}_H) - 2 \cdot \text{stdev}(\text{Data}_H)$

$\text{minus2sig} = 9.813$

B1.3. Statistical Analysis of Amplifier Voltage Response Data To Estimate Experimental Repeatability

3-inch diameter 4140 steel shaft.

$i := 0..7$

$$\text{Data}_A \equiv \begin{bmatrix} 0.994 \\ 1.06 \\ 1.12 \\ 1.08 \\ 1.11 \\ 1.07 \\ 0.972 \\ 1.10 \end{bmatrix}$$

$\text{mean}(\text{Data}_A) = 1.063$

$\text{stdev}(\text{Data}_A) = 0.05$

$\text{plus2sig} := \text{mean}(\text{Data}_A) + 2 \cdot \text{stdev}(\text{Data}_A)$

$\text{plus2sig} = 1.164$

$\text{minus2sig} := \text{mean}(\text{Data}_A) - 2 \cdot \text{stdev}(\text{Data}_A)$

$\text{minus2sig} = 0.963$

$$\text{Data}_B \equiv \begin{bmatrix} 2.21 \\ 2.12 \\ 2.24 \\ 1.97 \\ 2.09 \\ 2.16 \\ 2.27 \\ 2.19 \end{bmatrix}$$

$\text{mean}(\text{Data}_B) = 2.156$

$\text{stdev}(\text{Data}_B) = 0.09$

$\text{plus2sig} := \text{mean}(\text{Data}_B) + 2 \cdot \text{stdev}(\text{Data}_B)$

$\text{plus2sig} = 2.336$

$\text{minus2sig} := \text{mean}(\text{Data}_B) - 2 \cdot \text{stdev}(\text{Data}_B)$

$\text{minus2sig} = 1.977$

$$\text{Data}_C \equiv \begin{bmatrix} 3.03 \\ 3.01 \\ 2.84 \\ 3.00 \\ 2.92 \\ 2.88 \\ 2.97 \\ 2.86 \end{bmatrix}$$

$\text{mean}(\text{Data}_C) = 2.939$

$\text{stdev}(\text{Data}_C) = 0.069$

$\text{plus2sig} := \text{mean}(\text{Data}_C) + 2 \cdot \text{stdev}(\text{Data}_C)$

$\text{plus2sig} = 3.076$

$\text{minus2sig} := \text{mean}(\text{Data}_C) - 2 \cdot \text{stdev}(\text{Data}_C)$

$\text{minus2sig} = 2.801$

$$\text{Data}_D \equiv \begin{bmatrix} 3.52 \\ 3.47 \\ 3.57 \\ 3.72 \\ 3.63 \\ 3.54 \\ 3.69 \\ 3.57 \end{bmatrix}$$

$\text{mean}(\text{Data}_D) = 3.589$

$\text{stdev}(\text{Data}_D) = 0.08$

$\text{plus2sig} := \text{mean}(\text{Data}_D) + 2 \cdot \text{stdev}(\text{Data}_D)$

$\text{plus2sig} = 3.749$

$\text{minus2sig} := \text{mean}(\text{Data}_D) - 2 \cdot \text{stdev}(\text{Data}_D)$

$\text{minus2sig} = 3.429$

$$\text{Data}_E \equiv \begin{bmatrix} 4.22 \\ 4.17 \\ 4.09 \\ 4.02 \\ 4.18 \\ 4.16 \\ 4.14 \\ 4.10 \end{bmatrix}$$

$\text{mean}(\text{Data}_E) = 4.135$

$\text{stdev}(\text{Data}_E) = 0.059$

$\text{plus2sig} := \text{mean}(\text{Data}_E) + 2 \cdot \text{stdev}(\text{Data}_E)$

$\text{plus2sig} = 4.252$

$\text{minus2sig} := \text{mean}(\text{Data}_E) - 2 \cdot \text{stdev}(\text{Data}_E)$

$\text{minus2sig} = 4.018$

$$\text{Data}_F \equiv \begin{bmatrix} 4.77 \\ 4.69 \\ 4.88 \\ 4.91 \\ 4.75 \\ 4.83 \\ 4.92 \\ 4.84 \end{bmatrix}$$

$\text{mean}(\text{Data}_F) = 4.824$

$\text{stdev}(\text{Data}_F) = 0.076$

$\text{plus2sig} := \text{mean}(\text{Data}_F) + 2 \cdot \text{stdev}(\text{Data}_F)$

$\text{plus2sig} = 4.976$

$\text{minus2sig} := \text{mean}(\text{Data}_F) - 2 \cdot \text{stdev}(\text{Data}_F)$

$\text{minus2sig} = 4.671$

$$\text{Data}_G \equiv \begin{bmatrix} 5.77 \\ 5.45 \\ 5.52 \\ 5.62 \\ 5.73 \\ 5.49 \\ 5.64 \\ 5.85 \end{bmatrix}$$

$\text{mean}(\text{Data}_G) = 5.634$

$\text{stdev}(\text{Data}_G) = 0.133$

$\text{plus2sig} := \text{mean}(\text{Data}_G) + 2 \cdot \text{stdev}(\text{Data}_G)$

$\text{plus2sig} = 5.9$

$\text{minus2sig} := \text{mean}(\text{Data}_G) - 2 \cdot \text{stdev}(\text{Data}_G)$

$\text{minus2sig} = 5.367$

$$\text{Data}_H \equiv \begin{bmatrix} 6.67 \\ 6.52 \\ 6.72 \\ 6.38 \\ 6.51 \\ 6.44 \\ 6.59 \\ 6.47 \end{bmatrix}$$

$\text{mean}(\text{Data}_H) = 6.537$

$\text{stdev}(\text{Data}_H) = 0.108$

$\text{plus2sig} := \text{mean}(\text{Data}_H) + 2 \cdot \text{stdev}(\text{Data}_H)$

$\text{plus2sig} = 6.754$

$\text{minus2sig} := \text{mean}(\text{Data}_H) - 2 \cdot \text{stdev}(\text{Data}_H)$

$\text{minus2sig} = 6.321$

$$\text{Data}_I \equiv \begin{bmatrix} 7.47 \\ 7.36 \\ 7.53 \\ 7.29 \\ 7.39 \\ 7.32 \\ 7.50 \\ 7.43 \end{bmatrix}$$

$\text{mean}(\text{Data}_I) = 7.411$

$\text{stdev}(\text{Data}_I) = 0.081$

$\text{plus2sig} := \text{mean}(\text{Data}_I) + 2 \cdot \text{stdev}(\text{Data}_I)$

$\text{plus2sig} = 7.572$

$\text{minus2sig} := \text{mean}(\text{Data}_I) - 2 \cdot \text{stdev}(\text{Data}_I)$

$\text{minus2sig} = 7.25$

$$\text{Data}_J := \begin{bmatrix} 8.12 \\ 8.27 \\ 8.09 \\ 8.22 \\ 8.19 \\ 8.31 \\ 8.24 \\ 8.17 \end{bmatrix}$$

$\text{mean}(\text{Data}_J) = 8.201$

$\text{stdev}(\text{Data}_J) = 0.069$

$\text{plus2sig} := \text{mean}(\text{Data}_J) + 2 \cdot \text{stdev}(\text{Data}_J)$

$\text{plus2sig} = 8.34$

$\text{minus2sig} := \text{mean}(\text{Data}_J) - 2 \cdot \text{stdev}(\text{Data}_J)$

$\text{minus2sig} = 8.063$

$$\text{Data}_K := \begin{bmatrix} 8.88 \\ 9.36 \\ 9.08 \\ 9.21 \\ 9.04 \\ 9.27 \\ 9.11 \\ 9.17 \end{bmatrix}$$

$\text{mean}(\text{Data}_K) = 9.14$

$\text{stdev}(\text{Data}_K) = 0.138$

$\text{plus2sig} := \text{mean}(\text{Data}_K) + 2 \cdot \text{stdev}(\text{Data}_K)$

$\text{plus2sig} = 9.417$

$\text{minus2sig} := \text{mean}(\text{Data}_K) - 2 \cdot \text{stdev}(\text{Data}_K)$

$\text{minus2sig} = 8.863$

$$\text{Data}_L := \begin{bmatrix} 10.1 \\ 9.84 \\ 9.90 \\ 9.68 \\ 9.59 \\ 9.77 \\ 10.0 \\ 9.72 \end{bmatrix}$$

$\text{mean}(\text{Data}_L) = 9.825$

$\text{stdev}(\text{Data}_L) = 0.159$

$\text{plus2sig} := \text{mean}(\text{Data}_L) + 2 \cdot \text{stdev}(\text{Data}_L)$

$\text{plus2sig} = 10.143$

$\text{minus2sig} := \text{mean}(\text{Data}_L) - 2 \cdot \text{stdev}(\text{Data}_L)$

$\text{minus2sig} = 9.507$

$$\text{Data}_M := \begin{bmatrix} 10.7 \\ 10.3 \\ 10.4 \\ 9.98 \\ 10.2 \\ 10.2 \\ 10.5 \\ 10.0 \end{bmatrix}$$

$\text{mean}(\text{Data}_M) = 10.285$

$\text{stdev}(\text{Data}_M) = 0.229$

$\text{plus2sig} := \text{mean}(\text{Data}_M) + 2 \cdot \text{stdev}(\text{Data}_M)$

$\text{plus2sig} = 10.744$

$\text{minus2sig} := \text{mean}(\text{Data}_M) - 2 \cdot \text{stdev}(\text{Data}_M)$

$\text{minus2sig} = 9.826$